# Effects of Microneedle System on the Skin Permeation of Drugs

甲第35号

2007

Xueming Wu

# Effects of Microneedle System on the Skin Permeation of Drugs

2007

Xueming Wu

## Contents

## ABBREVIATIONS

| | |
|---|---|
| FDs | fluorescein isothiocyanate -dextrans |
| LDH | lactate dehydrogenase |
| i.p. | intraperitoneal |
| PBS | phosphate buffered saline |
| P | permeability coefficient |
| $R_t$ | total skin resistance |
| $R_{sc}$ | resistance of stratum corneum |
| $R_{ved}$ | resistance of viable epidermis and dermis |
| M.W. | molecular weight |
| IP | iontophoresis |
| $D_2O$ | deuterium oxide |
| $J$ | flux |
| $\Delta\mu$ | chemical potential difference |
| $\Delta E$ | voltage difference |
| $\Phi$ | dissipation function |
| $dS/d_t$ | inner entropy production per unit time |
| $\overline{V}$ | partial molar volume |
| $\Delta\pi$ | osmotic pressure difference |
| $\delta$ | reflection coefficient |

## Abstract

Microneedle systems have been paid attention as having many advantages over transdermal patches and hypodermic needles. The procedure provides adequate skin permeation rates without pain or severe infection. To obtain information for designing a microneedle system, the pretreatment effect of microneedle puncture in the skin barrier stratum corneum on the *in vitro* skin permeation of fluorescein isothiocyanate (FITC)-dextrans (4.3, 9.6 and 42.0 kDa) (FD-4, FD-10 and FD-40) was evaluated in hairless rats. The effect of sandpaper abrasion was also investigated for comparison. Both pretreatments on the skin barrier significantly increased the skin permeation of FDs. Lactate dehydrogenase (LDH) leaching was measured after the pretreatment of microneedle puncture and sandpaper abrasion on the skin barrier to evaluate the skin damage by these pretreatments. Lower leaching of LDH was observed after the microneedle puncture than after sandpaper abrasion. Next, a parallel permeation-resistance model of the skin barrier was established to see a relationship between number of microneedle puncture and enhancement effect on the skin permeation of drugs. Skin permeation of FD-10 could be predicted by the model as a function of the number of pores in the skin barrier. Our results suggest that the needle puncture may provide a safe, efficient and controllable alternative for increasing transdermal drug delivery.

Next, a combination of microneedle pretreatment and iontophoresis was evaluated for the potential to further increase skin permeation of drugs. Two model compounds with low and high molecular, $D_2O$ and FDs (FD-4, FD-10, FD-40, FD-70 and FD-2000; average molecular weight of 4.3, 9.6, 42.0, 71.2 and 2000 kDa), respectively, were used and the effect of microneedle pretreatment and iontophoresis on their *in vitro* permeability was evaluated using excised hairless rat skin with a modified 2-chamber diffusion cell. Convective solvent flow through the skin was measured using a set of calibrated capillaries attached to the diffusion cell. The following results were obtained: (1) convective solvent flow (electroosmosis) during iontophoresis through microneedle-pretreated skin, 2.62 ± 0.32 $\mu L/cm^2/h$, was almost the same as through intact skin, 2.71 ± 0.25 $\mu L/cm^2/h$, and (2) the

combination of microneedle pretreatment and subsequent iontophoresis significantly enhanced FD flux compared with microneedle pretreatment alone or iontophoresis alone, whereas no synergistic effect was found on the flux of $D_2O$. These results suggest that the combination of iontophoresis with microneedle pretreatment may be a useful means to further increase skin permeation of high molecular compounds.

Finally, linear phenomenological equations were applied to analyze drug transport phenomena through the microneedle-pretreated skin. They enable us better understanding and explanation to each contribution of passive diffusion and electroosmosis to the skin permeation of drugs. Applying the concept of reflection coefficient, we obtained a reasonable explanation to mechanism of the combined effects of microneedle pretreatment and iontophoresis on the skin permeation of high molecular compounds. These results suggest that the linear phenomenological equations are useful to mechanistically analyze permeability phenomena when a system contains more than two driving forces.

## General Introduction

Oral formulations of drugs such as tablets and capsules and injections are two of the main drug administration techniques. However, the use of tablets and capsules is not always feasible due to easy drug degradation in the gastrointestinal tract and possible first-pass effects in the liver. Injections are limited by pain at the injection site, possible infection during and after injection, and difficult self-administration. To avoid these problems, transdermal drug delivery has gradually gained attention as a third route of drug administration. It is difficult, however, to efficiently deliver therapeutically effective doses of drugs through the skin into the systemic circulation due to the large barrier function of the stratum corneum, the outermost layer of skin. To increase or improve the skin permeation of drugs, a variety of approaches have been studied such as combined use of chemical enhancers[1)] and physical means of iontophoresis[2)], electroporation[3)] and sonophoresis[4,5)]. Among them, electroporation generates nanometer-scale disruptions in the stratum corneum, which creates drug pathways through the skin barrier.

Recently, as an attractive alternative, the use of microneedles[6)], which have advantages over conventional needles and transdermal patches, has gained unprecedented attention for increasing the skin permeability of drugs. As compared to hypodermic needle injection, microneedles can provide a minimally invasive means of painless, precisely controlled and convenient delivery of therapeutic molecules into the skin, and the technique seldom causes infection[7)]. Furthermore, microneedles can create nanometer or micrometer-scale transport pathways sufficiently large enough to deliver macromolecules and even drug-loaded nanoparticles into the skin[6)]. So microneedles can be used not only to enhance transdermal delivery of small molecules, but also more importantly, to increase the skin permeation of macromolecules, such as proteins and DNA. Especially, for transdermal delivery of macromolecules microneedle system is considered a revolutionary technique, because other conventional enhancing methods mentioned as above cannot achieve.

On the other hand, transdermal iontophoresis has proved to increase the skin permeation of many molecules. Leduc had shown nearly 100 years ago that this technique could be used

to deliver active drugs across mammalian skin *in vivo*, but this did not gain scientific prominence until 20 years ago[8]. Iontophoretic flux is obtained not only due to electrorepulsion but also electroosmotic solvent flow, which is produced from anode to cathode by anodal iontophoresis. Thus, iontophoresis can be used to enhance transdermal delivery of ionic drugs as well as non-ionic compounds. To date, transdermal iontophoresis has obtained great success to increase skin permeation of many small molecules. The transport of large molecules, however, remains problematic[9].

In order to expand the range of drugs suitable for transdermal delivery, iontophoresis in combination with other means (iontophoresis + electroporation[10-14], iontophoresis + phonophoresis[5,15], iontophoresis + chemical enhancers[16-18] or iontophoresis + jet injector[19]) has already been tried. Although these combined methods increased transport rate of drugs through skin with varied levels of success, only several times increases were observed for the synergistic effects[20]. Since the microelectronics industry could fabricate uniform arrays of micron-scale needles, a rapid increase of interest was provoked in microneedle systems as a transdermal drug delivery system. However, few studies have reported on the combination of iontophoresis with microneedle technologies.

In view of the present study situation about microneedle and iontophoresis, we carried out the following experiments. In Chapter 1, the effects of pretreatment of microneedle puncture and sandpaper abrasion on the *in vitro* skin permeation of fluorescein isothiocyanate (FITC)-dextrans were investigated[21]. In Chapter 2, the enhancement of skin permeation of high molecular compounds by a combination of microneedle pretreatment and iontophoresis was investigated[22]. In Chapter 3, the enhancement of skin permeation of drugs was analyzed by using linear phenomenological equations.

# Chapter 1

## Effects of Pretreatment of Needle Puncture and Sandpaper Abrasion on the *In Vitro* Skin Permeation of Fluorescein Isothiocyanate (FITC)-Dextrans

### 1.1. Introduction

Since Henry et al.[23] first used microneedles as a transdermal drug delivery system, there has been a rapid increase of interest in microneedle systems[24]. The use of microneedles increased skin permeability of many molecules such as calcein[13], desmopressin[25], diclofenac[26], methyl nicotinate[27], bischloroethyl nitrosourea[28], insulin[26,29,30,31], bovine serum albumin[32], ovalbumin[33], oligodeoxynucleotide[34], plasma DNA[35], and particles such as polystyrene latex nanospheres[6,36], and gene therapy vectors[36], and so on. To our knowledge, however, little quantitative research has been performed for microneedle systems, such as those for determining a relationship between permeability and the number, size or length of microneedles. We therefore used a microneedle system made by ourselves to investigate the effects of pretreatment of needle puncture in the skin barrier on the *in vitro* skin permeation of macromolecules. The final objective of this study was to obtain quantitative information for designing microneedle systems. The relationship between the number of pores created by needle puncture and the drug permeability through the pretreatment skin barrier was studied using fluorescein isothiocyanate (FITC)-dextrans (4.3, 9.6 and 42.0 kDa) (FD-4, FD-10 and FD-40) as model compounds. The effect of sandpaper abrasion[37] was also investigated for comparison. Moreover, lactate dehydrogenase (LDH) leaching from the pretreated skin, which is a marker of skin viability[38], was determined as an index of skin damage by the microneedle system and sandpaper abrasion.

### 1.2. Materials and Methods

#### *1.2.1. Materials*

FITC-dextrans (FD-4, FD-10 and FD-40; average molecular weight, 4.3, 9.6 and 42.0

kDa, respectively) were purchased from Sigma Aldrich (St. Louis, MO, U.S.A.). Other reagents were of analytical grade and used without further purification.

*1.2.2. Preparation of microneedle for skin puncture*

In the needle puncture experiment in the skin barrier, a 27-gauge disposable hypodermic needle (i.d., 0.22 mm; o.d., 0.40 mm; Terumo Co., Tokyo, Japan) was used. The needle was covered with polyethylene tubing (PE-50; i.d., 0.58 mm; o.d., 0.97 mm; Hibiki, Tokyo, Japan) as a needle sheath to maintain constant insertion depth in the skin barrier, as shown in Fig. 1-1. The PE-50 cover allows only insertion of the needle tip (about 160 μm length) into the skin.

*1.2.3. Experimental animals*

Male hairless rats (WBM/ILA-Ht, 7-9 weeks-old, body weight: 180-250 g) were purchased either from Life Science Research Center, Josai University (Sakado, Saitama, Japan) or Ishikawa Experimental Animal Laboratories (Fukaya, Saitama, Japan). They were housed in temperature-controlled rooms (25 ± 2°C) with a 12-h light-dark cycle (07:00-19:00 h). The rats were allowed free access to food (M.F. Oriental, Tokyo, Japan) and tap water for a week before experiments began. Every animal experiment was conducted under the guidelines of the Life Science Research Center at Josai University.

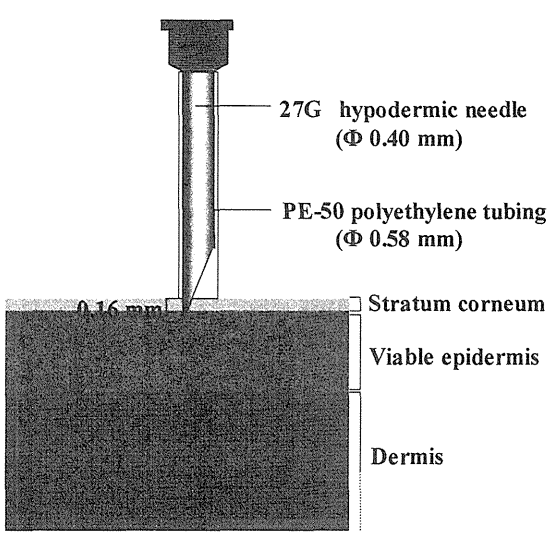


Fig. 1-1. Schematic representation of needle puncture on skin surface with a hypodermic needle.

*1.2.4. Pretreatment of skin*

Abdominal full-thickness skin of hairless rats was excised under anesthesia by *i.p.* injection of sodium pentobarbital (50 mg/kg) and excess subcutaneous fat was carefully eliminated.

*1.2.4.1. Puncturing with a 27-gauge hypodermic needle*

The excised skin was punctured with a 27-gauge hypodermic needle with the PE-50 sheath (see Fig. 1-1). The number of punctures with a depth of about 160 μm was set to be one, three, nine or *n* in the stratum corneum.

*1.2.4.2. Abrading with sandpaper*

The excised skin surface was gently abraded once with sandpaper of No.600 (Sankyo Rikagaku Co., Okegawa, Saitama, Japan). In order to maintain constant abrasion strength, the technique was practiced at length until an acceptable repeatability was reached.

*1.2.4.3. Stripping the stratum corneum with adhesive tape*

The stratum corneum of the excised skin was stripped with adhesive tape (Scotch Magic Transparent Tape®, 3M Co., Minneapolis, MN, U.S.A.) about 20 times, until the stratum corneum was entirely removed from the skin.

*1.2.5. In vitro skin permeation study*

The skin pretreated with needle puncture or sandpaper abrasion was mounted in a vertical diffusion cell with an effective diffusion area of 1.77 $cm^2$. Intact full-thickness skin and stripped skin were also used for comparison[39]. A test solution (1.0 mL) containing 0.25 mM FD-4, FD-10 or FD-40 was placed on the stratum corneum side of the skin. The receiver solution was 6.0 mL of pH 7.4 phosphate buffered saline (PBS), which was maintained at 32°C using a thermo-regulated water bath. A magnetic stirrer bar was added in the receiver compartment, which stirred at about 1200 rpm throughout the experiment.

The cell set is shown in Fig. 1-2. The receiver solution (0.4 mL) was withdrawn every 1 h, and the same volume of PBS was added to the receiver compartment to keep the volume constant. Every permeation-run was repeated 3 to 5 times.

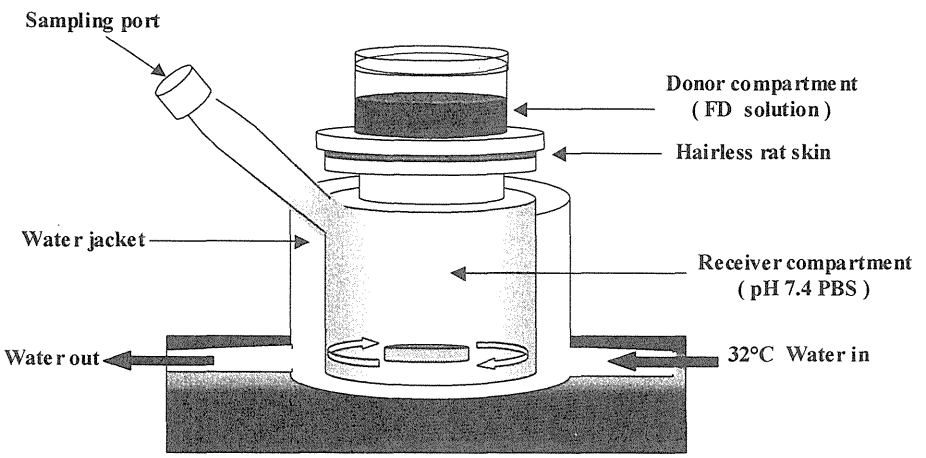


Fig. 1-2. Experimental set-up for *in vitro* permeation study

*1.2.6. Assay of FITC-Dextrans*

The concentration of FD-4, FD-10 and FD-40 in each receiver sample was determined using a spectrofluorophotometer (RF 5300PC, Shimadzu, Kyoto, Japan) at an excitation wavelength of 495 nm and fluorescent emission wavelength of 515 nm.

*1.2.7. Measurement of lactate dehydrogenase leached from pretreated skin*

Skin that had been pretreated with needle puncture or sandpaper abrasion was loaded into a vertical diffusion cell, with the stratum corneum side facing the receiver compartment. The receiver compartment was filled with PBS (6.0mL), which was continuously stirred by a magnetic stirrer bar and was thermo-regulated with a water jacket at 32°C. The upside compartment (dermis side) was also filled with 1 mL of PBS to avoid the dermis side becoming dry. Samples were withdrawn from the receiver compartment at predetermined time intervals. LDH leached from the stratum corneum side was determined by an assay kit (Lactate Dehydrogenase Kit, Wako Pure Chemicals, Osaka, Japan). All experiments were carried out at least in triplicate.

## 1.3. Theoretical

A parallel skin permeation-resistance model was established to evaluate a relationship between skin permeability and the number of pores made by needle puncture. According to skin anatomy and barrier function, skin is generally divided into two or three different layers: stratum corneum, viable epidermis and dermis. The most upper epidermis, the stratum corneum, is considered to be the primary barrier to drug transport through the skin. Then the total skin resistance ($R_t$), where permeation resistance, $R$, is represented as the reciprocal of the permeability coefficient ($1/P$), and may be composed of resistances in the stratum corneum ($R_{sc}$) and viable epidermis and dermis ($R_{ved}$), as shown in Fig. 1-3a and in eqn. 1.

$$R_t = R_{sc} + R_{ved} \tag{1}$$

where $R_t$ and $R_{ved}$ are obtained from permeation experiments using intact skin and stripped skin, respectively. Thus, $R_{sc}$ is the difference between $R_t$ and $R_{ved}$. Furthermore, $R_{sc}$ and $R_{ved}$ can be considered to be the sum of $m$ numbers of the same resistance $r_{sc}$ and $r_{ved}$ by a parallel connection, as illustrated in Fig. 1-3b. The relationship between $R_t$ and $r_{sc}$, $r_{ved}$ is:

$$\frac{1}{R_t} = \frac{1}{r_{sc} + r_{ved}} + \frac{1}{r_{sc} + r_{ved}} + \bullet\bullet\bullet + \frac{1}{r_{sc} + r_{ved}} = \frac{m}{r_{sc} + r_{ved}} \tag{2}$$

$$r_{sc} = mR_{sc}, r_{ved} = mR_{ved} \tag{3}$$

where $r_{sc}$, $r_{ved}$ and $m$ are dependent on pore properties, i.e., size and depth. When skin is punctured $n$ times, the total skin resistance, $R'_t$, can be represented as follows (see Fig. 1-3c):

$$\frac{1}{R'_t} = \frac{1}{r_{ved}} + \bullet\bullet\bullet + \frac{1}{r_{ved}} + \frac{1}{r_{sc} + r_{ved}} + \bullet\bullet\bullet + \frac{1}{r_{sc} + r_{ved}} = \frac{n}{r_{ved}} + \frac{m-n}{r_{sc} + r_{ved}} \tag{4}$$

Introducing $R_{sc}$ and $R_{ved}$ from eqn. (3) and rearranging terms, $R'_t$ becomes:

$$R_t' = \frac{m \bullet R_t \bullet R_{ved}}{n \bullet R_{sc} + m \bullet R_{ved}} \tag{5}$$

Then the permeability coefficient of total skin after being punctured n times,

$$P_t' = \frac{1}{R_t'} = \frac{n \bullet R_{sc} + m \bullet R_{ved}}{m \bullet R_t \bullet R_{ved}} \tag{6}$$

a)

b)

c)

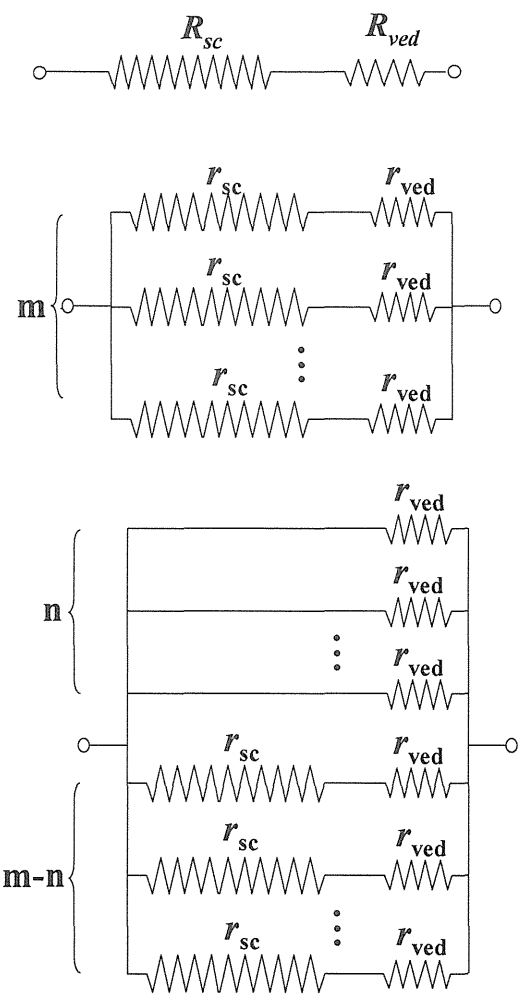


Fig. 1-3. Schematic representation of a skin permeation-resistance model. a: Resistance model for intact skin; b: Parallel resistance model for intact skin; c: Resistance model for punctured skin.

## 1.4. Results and Discussion

### *1.4.1. Effect of pretreatment (needle puncture and sandpaper abrasion) on the skin permeation of FD-10*

To assess the ability of physical pretreatments of needle puncture, sandpaper abrasion and tape stripping for increasing skin permeation of drugs, the permeability of FD-10 through excised hairless rat skin was determined using a vertical diffusion cell. The obtained results are shown in Fig. 1-4. The cumulative amounts of FD-10 that permeated through skin showed a typical time course, i.e., short lag time and a following pseudo-steady state flux, independent of the pretreatment methods.

The passive permeability coefficient of FD-10 across intact skin was $2.67 \times 10^{-10}$ cm/s. Puncturing three pores across the surface of skin barrier (pore-3, 3 pores-group) enhanced the permeability by more than 10-fold ($3.70 \times 10^{-9}$ cm/s). In this needle puncture experiment, the skin barrier was partly damaged by three times of local puncture. The permeability coefficient of FD-10 through the skin was also significantly increased by sandpaper abrasion (sandpaper-1, one treatment with sandpaper) ($6.65 \times 10^{-9}$ cm/s). However, the stripped skin permeability ($8.25 \times 10^{-7}$ cm/s) was much higher. Thus, the permeations of FD-10 through skin treated with needle puncture and sandpaper abrasion were much higher than the passive permeation through intact skin, but was much lower when compared with stripped skin. These results suggest that the present physical penetration-enhancing methods have an effect mainly on the barrier function of the stratum corneum.

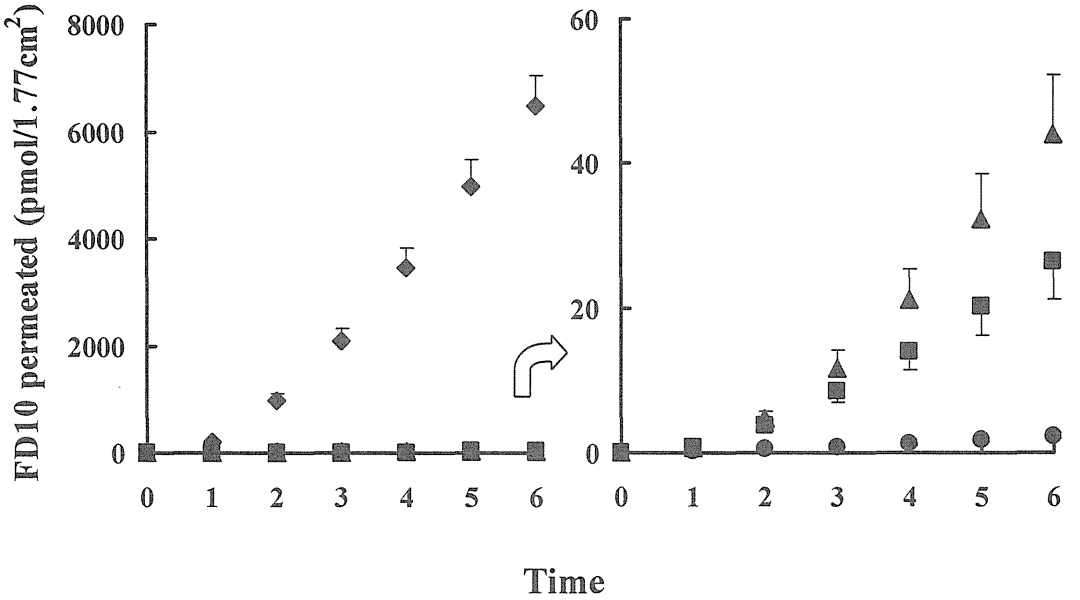


Fig. 1-4. Effect of different pretreatments on skin permeation of FD-10.

Symbols: ●, Intact skin; ■, Needle puncture (pore-3); ▲, Sandpaper abrasion (sandpaper-1); ♦, Tape stripping. Each point represents the mean ± S.E. of 3 or 4 experiments.

*1.4.2. Relationship between P and M.W.*

In order to further study the effect of needle puncture, sandpaper abrasion and tape stripping on the macromolecular permeation through hairless rat skin, a relationship was investigated between the permeability coefficient (*P*) through the treated skin and molecular weight (*M.W.*) of the penetrants. Skin permeations of FD-4 and FD-40 were also determined.

In all experiments, *P* after these pretreatments decreased with an increase in *M.W.* of the penetrants as shown in Fig. 1-5. In addition, relatively good linear correlations were observed between Log *M.W.* and Log *P*, which coincided with the previous report by Baker and Lonsdale[40]. Interestingly, a similar enhancement effect was observed by pretreatments with pore-3 and sandpaper-1.

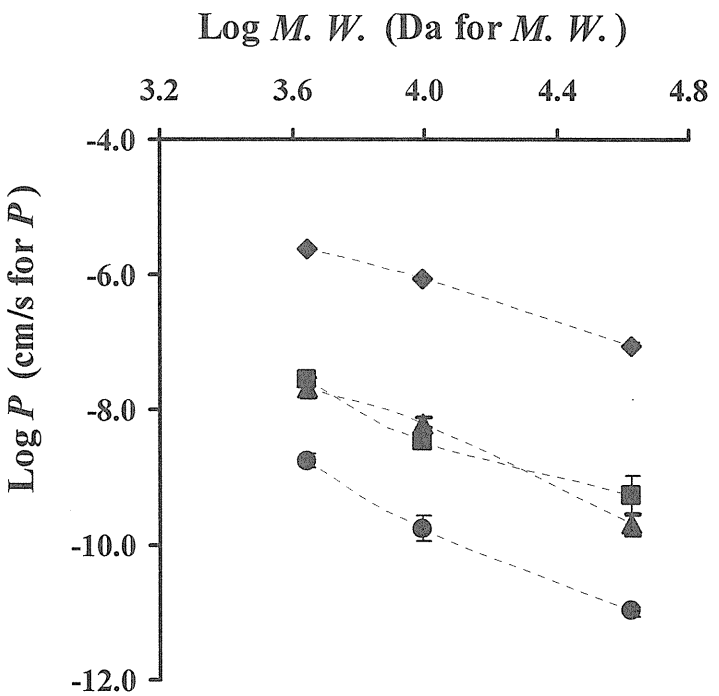


Fig. 1-5. Relationship between Log *P* and Log *M.W.* of FD-4, FD-10 and FD-40. Symbols: the same in Fig. 1-4. Each point represents the mean ± S.E. of 3 or 4 experiments.

Figure 1-6 summarizes the enhancing ratio of skin permeation of FDs by the present pretreatments. It is very important to consider that the enhancing ratio for the skin permeation of FDs by the present pretreatments was more marked for higher M.W. FDs. This is probably due to different permeation pathways that exist for penetrants with different molecular sizes. Low molecular compounds primarily permeate the actual stratum corneum (probably intercellular lipid domain between corneocytes), whereas high molecular compounds may diffuse the pore region (containing hair follicles), as initially stated by Scheuplein[41]. Only a few pathways are available for the permeation of the largest model compound in the present study, FD-40 through the intact skin, whereas relatively more pathways are available for the skin permeation of FD-4. When decreasing the skin barrier function by physical means such as needle puncture and sandpaper abrasion, the permeation pathway, especially for high molecular weight compounds, may be produced in the stratum corneum.

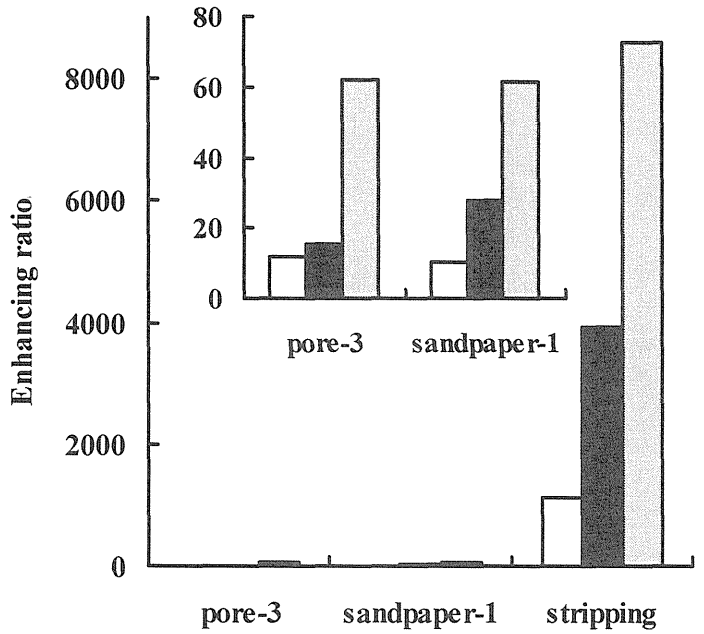


Fig. 1-6. The effect of different pretreatments on the enhancing ratio of skin permeation of FD-4, FD-10 and FD-40. Symbols: opened column, FD-4; closed column, FD-10; shadowed column, FD-40. Each column represents the mean value (the mean permeability of pretreatment against the mean permeability of control)

*1.4.3. Effect of number of pores made by needle puncture on the skin permeability of FD-10*

Needle puncture and sandpaper abrasion were shown to effectively improve permeability of high molecular weight compounds through hairless rat skin. They were insufficient, however, compared to tape stripping (*P* for pore-3 or sandpaper-1 was about 1/100 of stripped skin). Thus, the skin permeation of FD-10 was further examined by increasing the number of pores made by needle puncture. The experimental results are shown in Fig. 1-7. Skin permeation increased as the number of pores increased. However, the skin permeation was not strictly proportional to the number of pores.

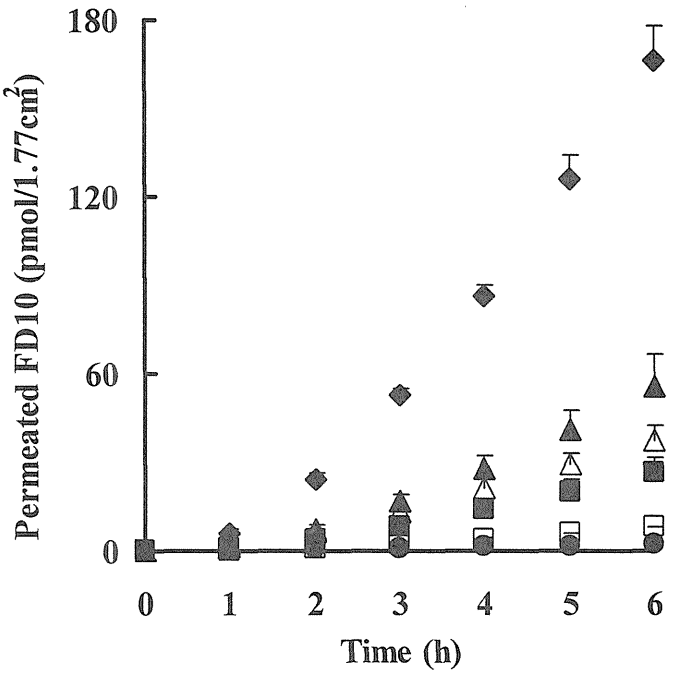


Fig. 1-7. Effect of pore number on the skin permeation of FD-10.

Symbols: ●, Intact skin; □, Pore-1; ■, Pore-3; △, Pore-6; ▲, Pore-9; ♦, Pore-25. Each point represents the mean ± S.E. of 3 or 4 experiments. Pore-number shows the number of needle puncture into the skin surface.

We then established a parallel permeation-resistance model representing skin permeation profiles to predict skin permeation of drugs after needle puncture pretreatment (see Theoretical). Fig. 1-8 shows relationship between $P$ (calculated by skin permeation data of FD-10) and the number of pores made in the stratum corneum. Predictions using the skin permeation-resistance model were in agreement with the experimental data. In this calculation, $R_{sc}$ and $R_{ved}$ are fixed to $4.20 \times 10^9$ s/cm and $1.07 \times 10^6$ s/cm, respectively, from the experimental data. The parameter $m$ was calculated to be about 1500, by curve-fitting of a set of the obtained $R'_t$ and $n$ to eqn. 6 using the least-squares method (Microsoft Excel, Solver: algorithm, quasi Newton method). This means that the skin permeation would be enhanced to the maximum value, which was comparable to that of stripped skin, when about 1500 pores were made within the area of $1.77cm^2$ in the stratum corneum with ourselves-made microneedle. As a function of the pore number, the skin permeation can be

predicted by eqn. (6). Although additional studies are necessary to clarify the effects of size, length and other properties of needle puncture on the skin resistance, the obtained results suggest a strong possibility of this permeation-resistance model to predict skin permeability. Furthermore, even a skin permeability treated with a new microneedle system can also be predicted by extrapolation from a given microneedle-treated skin permeability through modifying the parameters in eqn. (6).

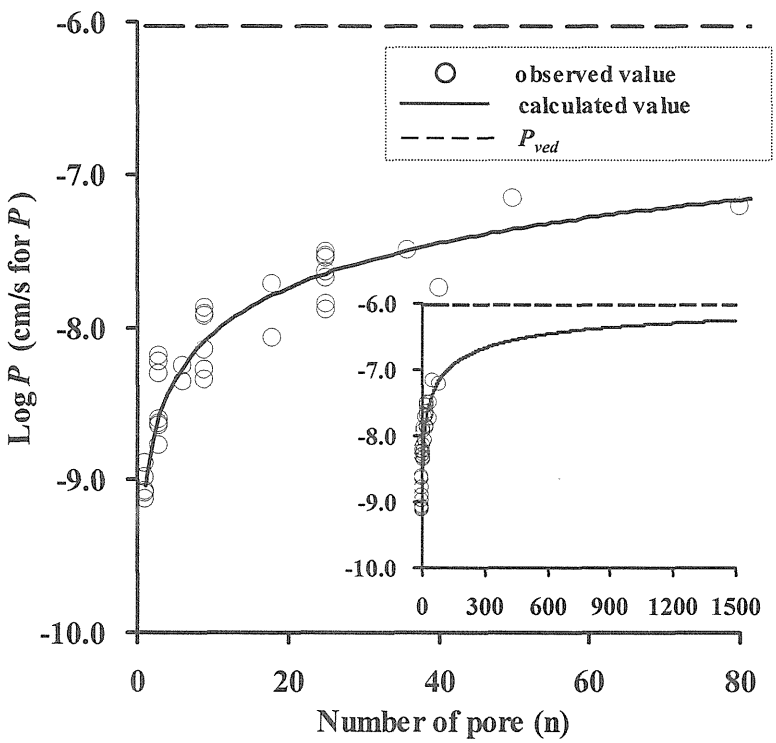


Fig. 1-8. Observed and calculated log ($P$) of FD-10 with different number of pores. Symbols: ○, Observed value; —, Curve-fitting line

*1.4.4. LDH activity of pretreated skin*

The safety investigation of microneedles is rarely involved except a study reported by Kaushik et al.[7]. They used visual analog pain scores to evaluate the safety of microneedle and suggested that microneedles could provide a useful clinical tool for minimally invasive drug delivery. However, more precise evaluation methods have not been developed. Then, as a marker of skin viability, the activity of LDH leached from the skin barrier pretreated by different physical enhancing methods was evaluated to assess skin viability[38]. Fig. 1-9

shows the obtained data. In all pretreatments, LDH leached from the skin surface increased with the passage of time. Comparison of pore-3 to sandpaper-1, where the enhancing effect by both methods was almost the same, showed that LDH activity for the pore-3 was significantly lower than that for sandpaper-1, suggesting that skin damage caused by needle puncture was much lower compared to the sandpaper abrasion, and that needle puncture must be more effective and safe to enhance skin permeation of drugs.

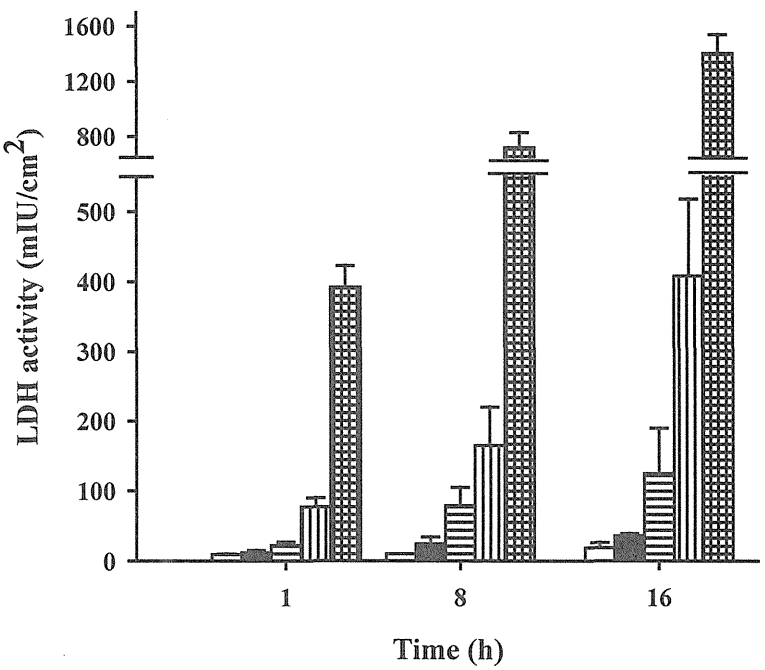


Fig. 1-9. Effect of different pretreatments on the LDH leaching from the skin surface. Symbols: □, Intact skin; ■, Needle puncture (pore-3); ═, Needle puncture (pore-50); ▥, Sandpaper abrasion (sandpaper-1); ╫, Tape stripping. Each point represents the mean ± S.E. of 3 or 4 experiments.

### 1.5. Chapter Conclusion

The present study demonstrated that microneedle pretreatment is capable of effective delivery of macromolecules through skin. It is of great significance in the transdermal drug delivery systems, because a revolutionary development was obtained for transdermal delivery of macromolecules, such as proteins and DNA, which other enhancing methods cannot

succeed. Measurement of LDH leaching shows that needle puncture to the stratum corneum is much safer than sandpaper abrasion. These results may support the concept that microneedles provide a safe and efficient alternative for minimally invasive transdermal drug delivery. Using a parallel permeation-resistance model, skin permeability after needle puncture can be predicted as a function of pore number. Although further studies are needed concerning the resistance model, these preliminary results exhibit a strong possibility of precise prediction and control of skin permeability with microneedle systems.

In spite of many advantages of microneedle system as mentioned above, the skin permeation rate introduced only by the microneedle pretreatment was very small compared with that through stratum corneum-stripped skin. In order to obtain high permeation, making many pores in skin is easily considered since the permeation was dependent on the pretreated-number or area of stratum corneum. However, on the other hand, the more pores being made in the stratum corneum, the greater irritation of skin will be deduced. So we must find out an effective approach under safe condition. In the next chapter, we have an attempt to develop a combination method of microneedle pretreatment and iontophoresis.

# Chapter 2

## Enhancement of Skin Permeation of High Molecular Compounds by A Combination of Microneedle Pretreatment and Iontophoresis

### 2.1. Introduction

In order to overcome the formidable barrier of the stratum corneum to drug permeation, several skin penetration-enhancing strategies have been developed by physical means such as iontophoresis[42], electroporation[43], phonophoresis[44] and microneedles[23]. Among them, microneedles can provide a minimally invasive and relatively safe means of painless, precisely controlled and convenient delivery of therapeutic molecules into the skin[6,7,23]. In our previous study[21], we evaluated lactose dehydrogenase (LDH) release, a means to evaluate the skin irritation, from skin surface in hairless rats, and found that the LDH release from skin surface pretreated with needle puncture was much lower than that with sandpaper abrasion. In addition, the needle puncture to rat skin markedly increased the skin permeability of FITC-dextrans. Furthermore, a newly developed parallel permeation-resistance model was useful to predict the effect of needle-pretreatment on the skin permeation. Thus, the permeation was fairly dependent on the pretreated-area of stratum corneum. Unfortunately however, the skin permeation rate introduced by microneedle pretreatment was very low compared with that through stratum corneum-stripped skin. This is because only a small diffusion area can be produced in the stratum corneum barrier by microneedles. Information can be obtained from traditional or conventional injection. It is necessary to pump a syringe using push pressure during drug administration by conventional injection, so much more effective transdermal delivery may be obtained if an osmotic device is used in conjunction with the microneedle delivery system.

Transdermal iontophoresis is available to increase the skin permeation of many molecules. Iontophoretic flux is obtained not only due to electrorepulsion but also electroosmotic solvent flow, which is produced from anode to cathode by anodal

iontophoresis. Thus, iontophoresis can be used to enhance transdermal delivery of ionic drugs as well as non-ionic compounds. In the present study, iontophoresis-induced electroosmotic flow, electroosmosis, was combined with microneedle drug delivery as a 'push force'. The problem is now whether the electrical properties of skin, which is the origin of electroosmotic flow[45], are affected by microneedle pretreatment. Physical abrasion of the stratum corneum and application of depilatory cream on skin surface can facilitate the iontophoretic delivery of insulin[46,47]. On the other hand, removal of the stratum corneum by tape stripping decreased or even abolished the skin electroosmotic flow[48]. Hirsch et al. also reported that iontophoresis on stripped skin did not result in a higher delivery than iontophoresis alone[49]. The question whether iontophoresis in conjunction with physical impairment of the skin barrier can further enhance the transdermal delivery of high molecular compounds must therefore be related to the electrical properties of skin, i.e. electroosmotic flow after pretreatment.

Since microneedles can provide a minimally invasive means of delivery of therapeutic molecules into skin and our previous study has also showed very low skin damage caused by needle puncture[21], the combination of barrier impairment using microneedles and following iontophoresis can be expected as a means to broaden the range of drugs suitable for transdermal delivery; however, few studies have reported on the combination of iontophoresis with microneedle technologies.

Thus, in this chapter, iontophoresis-induced electroosmotic flow, electroosmosis, was combined with microneedle drug delivery as a 'push force'. In detail, the purposes of the present study are: (1) to determine whether pretreatment with microneedles affects electroosmotic flow through hairless skin produced by iontophoresis; (2) to compare microneedle-pretreated skin permeability before and after iontophoresis; and (3) to examine microneedle-pretreated skin permeation characteristics of high molecular compounds.

## 2.2. Materials and Methods

### *2.2.1. Chemicals and electrodes*

Fluorescein isothiocyanate (FITC)-dextrans (FD-4, FD-10, FD-40, FD-70 and FD-2000; average molecular weight of 4.3, 9.6, 42.0, 71.2 and 2000 kDa) were used as model high molecular compounds. Deuterium oxide ($D_2O$) was also selected as a penetrant for comparison. FD-4, FD-10, FD-40, FD-70 and FD-2000 were purchased from Sigma Aldrich (St. Louis, MO, U.S.A.). $D_2O$ (99.9%, NMR grade), sodium chloride (NaCl), disodium hydrogen phosphate ($Na_2HPO_4$), and potassium dihydrogen phosphate ($KH_2PO4$) were obtained from Wako Pure Chemical Industries (Osaka, Japan). Silver wire (1.0 mm in diameter) was purchased from Matsumura Gold & Silver Co., Ltd. (Tokyo, Japan).

Ag/AgCl electrodes were used in all iontophoresis experiments. About 30 cm pure silver wire (1.0 mm diameter) was first cleaned with fine emery paper and one end was manipulated into a spiral loop as an Ag anode. The AgCl electrode was prepared by chloridizing the spiral silver wire immersed in 133 mM NaCl (silver plate cathode) at an applied current of about 50 mA for approximately 30 min.

### *2.2.2. Animals*

The animals used in this experiment were the same as described in Chapter 1.

### *2.2.3. Puncturing with microneedle array*

The excised skin was punctured with microneedle array tape, which contained 9 acupuncture needles (Haruhari, Taiho Medical Products Co., Ltd., Hiroshima, Japan) on a silicone sheet (1.0 × 20 × 20 mm, Togawa Rubber Co., Ltd., Tokushima, Japan), as shown in Fig. 2-1. Each needle tapered over a 400-μm length to a sharp tip with 28° angle, and the base diameter was approximately 200 μm. The microneedle array tape was manually pressed onto the rat skin, with the stratum corneum facing uppermost, at an approximate pressure of 1.6 kg/cm$^2$ for 10 s.

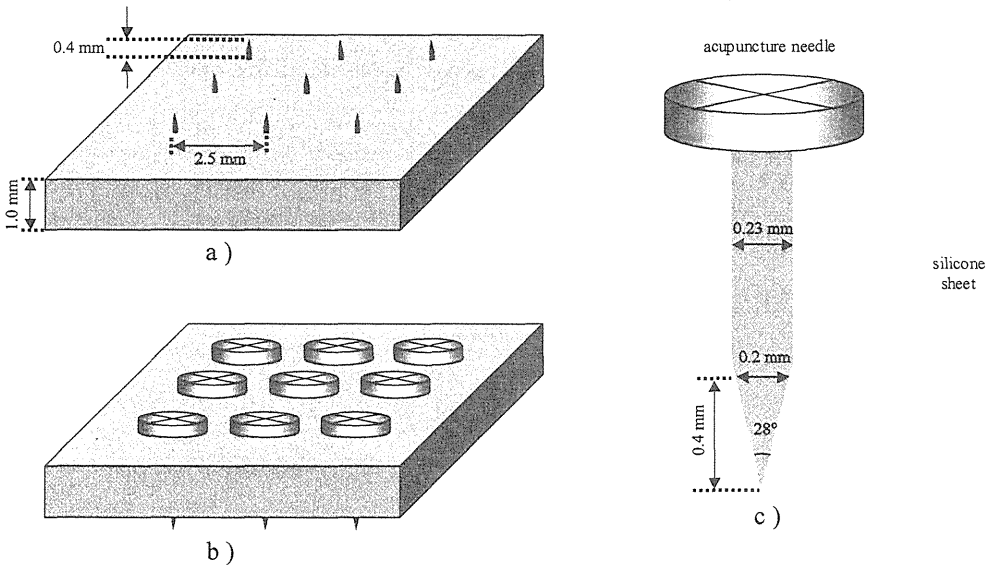


Fig. 2-1. Schematic illustration of microneedle array made by acupuncture needles. a) Top view, b) Back view, c) One needle.

*2.2.4. In vitro skin permeation study*

The excised skin membrane was mounted between two chambers of side-by-side diffusion cells (each 5.0 mL in volume and 0.95 $cm^2$ in effective diffusion area) (Fig. 2-2) for iontophoresis to conduct the permeation experiment. The stratum corneum side of the skin faced the drug donor chamber. FD-4, FD-10, FD-40 FD-70 or FD-2000 (1.0 mg/mL) in 1/30 M phosphate-buffered saline (PBS, pH 7.4) was added to the donor side and PBS alone was added to the receiver side. In $D_2O$ permeation experiments, $D_2O$ was added to the donor cell instead of FD solution.

Passive transport was first monitored for 5 h as a pre-iontophoretic period. A constant current of 0.29 mA (0.3 $mA/cm^2$) was then delivered to the electrodes for the next 5 h, with the anode and cathode in the donor and receiver compartments, respectively, during the iontophoretic period. After termination of the current, post-iontophoretic passive transport was measured for a further 5 h.

Both donor and receiver compartments were stirred with a magnetic stirrer bar driven by a constant-speed synchronous motor at about 1200 rpm and maintained at 32°C using a thermo-regulated water bath throughout the experiment. The receiver solution (0.4 mL) was withdrawn every 1 h, and the same volume of PBS was added to the receiver compartment to keep the volume constant. Each permeation experiment was repeated 3 to 5 times.

*2.2.5. Measurement of electroosmotic volume flow*

The diffusion cell was modified according to Pikal[50] and Kobatake[51] in order to directly measure volume flow across the skin, as shown in Fig. 2-2. Briefly, the excised skin was sandwiched between two Teflon mesh plates (0.5 mm thickness) with numerous 1.0 mm diameter holes. These plates prevent volume changes, which would result from deformation of the excised skin throughout the experiment, and yet allow the entire skin area to be available for the solvent and drug transport. The skin and two Teflon mesh plates were clamped between two chambers of side-by-side diffusion cells for iontophoresis (as above). The conditions of iontophoresis were also as above. Two horizontal 1.0-mm-diameter capillary tubes were attached via a silicone plug. The whole system was equilibrated, usually for about 1 h, until it was stabilized (movement of the solution meniscus in each capillary tube was minimal). The permeation experiment was then started by recording the position of each meniscus as a function of time. The electroosmotic volume flow, $J_v$, was calculated as follows:

$$J_v = v \times \left(\frac{S_{capillary}}{S_{skin}}\right)$$

where $v$ is electroosmotic solvent velocity, and $S_{capillary}$ and $S_{skin}$ are inner areas of capillary tubes and effective penetration area of skin, respectively.

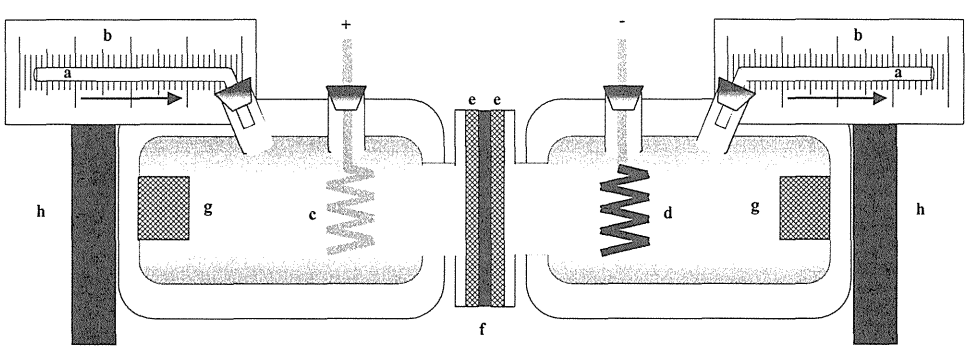


Fig. 2-2. Schematic illustration of diffusion cell used to measure solvent volume flow. a. capillary tube having an inner diameter of 1.0 mm; b. calibrated paper; c and d. Ag/AgCl electrodes (anode and cathode); e. Teflon mesh of 0.5 mm thickness and several holes of 1.0 mm diameter; f. excised hairless rat skin; g. magnetic stirrer bar; h. magnetic stirrer.

*2.2.6. Quantitative analysis*

FD-4, FD-10, FD-40, FD-70 and FD-2000 were analyzed by the method used in our previous study[21]. $D_2O$ was determined by measurement of the intensity of the O-D stretching vibrational band at 2512 $cm^{-1}$ infrared spectroscopic spectra[52].

## 2.3. Theoretic

The overall iontophoretic flux of a drug, $J_{total}$, is expressed as

$$J_{total} = J_{electrorepulsion} + J_{electroosmosis} + J_{passive} \quad (1)$$

where $J_{electrorepulsion}$, $J_{electroosmosis}$ and $J_{passive}$ are the flux due to electrorepulsion between the applied penetrant ion and electric field, convective solvent flow produced by electroosmosis and passive delivery through the skin, respectively. According to Pikal[45], Yoshida and Roberts[53], and Guy et al.[54], the relative importance of the three mechanisms in flux enhancement by iontophoresis strongly depends on the size of drug ions. The ionic effect dominates flux enhancement for small ions, whereas electroosmotic flow may dominate for the skin permeation of large ions such as peptides and proteins. Increased skin permeability by iontophoresis is thus generally marked not only for small ions but also for large ions. According to the free volume model by Yoshida and Roberts[53], the driving force for the delivery of ions having a molal volume of more than 2,000 will only be electroosmotic flow at iontophoresis. Pikal[45] also predicted that electroosmotic flow is the dominant mechanism for iontophoretic skin permeation of monovalent ions with Stokes radii larger than about 1 nm. Electrorepulsion flux was therefore assumed to be negligible for large molecules as follows:

$$J_{total} = J_{electroosmosis} + J_{passive} \quad (2)$$

In case of a combination of microneedle pretreatment and iontophresis, microneedle pretreatment produces new pores and enhances the skin permeability itself. Furthermore, solvent flow produced by electroosmosis facilitates the passage of high molecular compounds

through the new pores produced by the microneedle system. So a synergistic effect is expected by a combination of microneedle pretreatment and iontophoresis.

## 2.4. Results and Discussion

### *2.4.1. Pretreatment effect of microneedles on solvent volume flow through skin*

Since the electrical properties of skin are closely related to transdermal iontophoretic delivery[45,48], volume flow was firstly determined before and after microneedle pretreatment. No significant decrease was found in solvent volume flow for 1/30M PBS at pH7.4 (Fig. 2-3) after microneedle pretreatment, indicating that it did not change the electrical properties of skin, unlike stripping the stratum corneum[48,49]. When 1.0 mg/mL FDs was added to 1/30M PBS, volume flow was almost the same as that of PBS (data not shown).

Volume flow remained constant during 5 h iontophoresis. This is different from results reported by Pikal[50], in which a decrease in volume flow was observed over a long period of time. High current density (1.0 or 2.0 mA/cm$^2$) and low pH (pH 3.8) may change the electrical properties of skin to make the membrane charge weak, disappear or reverse. In the present experiments, however, the electrical properties of skin were not changed under modest conditions such as current density of 0.3 mA/cm$^2$ and pH 7.4.

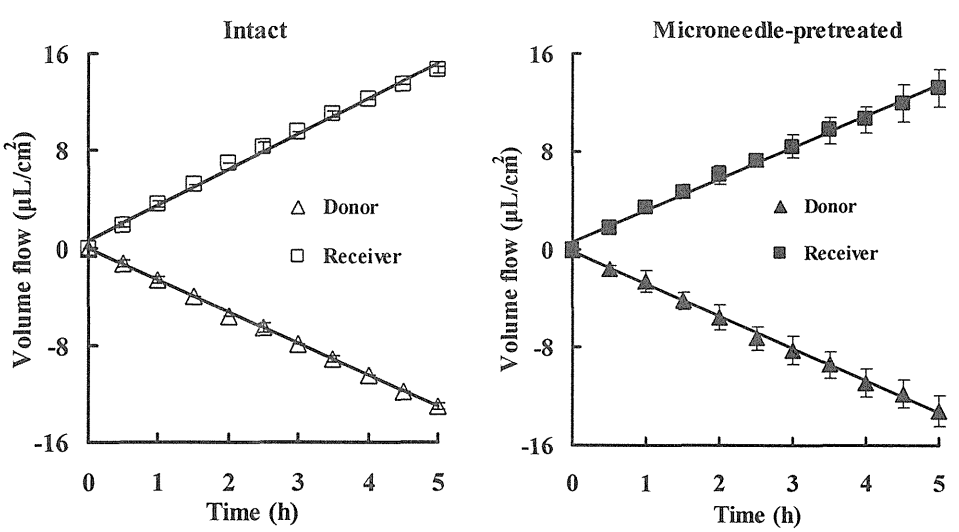


Fig. 2-3. Typical electroosmotic flow through excised hairless rat skin. Each panel shows volume flow in capillary tubes as a function of time. Left panel is intact skin, right panel is microneedle-pretreated skin.

*2.4.2. Pretreatment effect of microneedles on the skin permeation of $D_2O$*

Since no effect was observed on solvent volume flow by microneedle pretreatment, a combination of microneedle pretreatment and subsequent iontophoresis would be expected to further enhance the transdermal delivery of high molecular compounds. Passive flux through fresh intact skin (passive1), iontophoretic flux during iontophoresis (IP), and passive flux post-iontophoresis (passive2) of $D_2O$, as a model small molecule, are shown in Fig. 2-4 (left). After pretreatment, no significant increase was observed in the electroosmotic transport of $D_2O$. Flux due to electroosmotic transport[50], i.e., the flux difference between IP and passive2 is,

$$Electroosmotic \quad flow = Flux_{IP} - Flux_{passive2}$$

Electroosmotic flow was 2.45 and 2.67 μL/cm$^2$/h through the intact skin and microneedle-pretreated skin, respectively. The electroosmotic transport of $D_2O$ was almost the same as solvent volume flow measured by the capillary tube method (see Fig. 2-3). In addition, post-iontophoresis passive flux (passive2) was also high compared to passive1 permeability, and this permeability increase may be evaluated by the permeability factor, which was calculated from the ratio of passive2 to passive1 flux as follows[50]:

$$Permeability \quad factor = \frac{Flux_{passive2}}{Flux_{passive1}}$$

In the present experiment, permeability factors of intact skin and microneedle-pretreated skin were 1.19 and 1.65, respectively (Table 2-1).

*2.4.3. Pretreatment effect of microneedles on the skin permeation of FD-10*

We subsequently investigated the pretreatment effect of microneedles on the skin permeation of a large model molecule FD-10 (Fig. 2-4, right; Table 2-2). Iontophroresis did not contribute to FD10 transport through the intact skin. However, microneedle pretreatment significantly increased the electroosmotic transport of FD10, suggesting that high synergistic enhancing effects on the skin permeation of high molecular compounds could be obtained by a combination of microneedle pretreatment and iontophoresis.

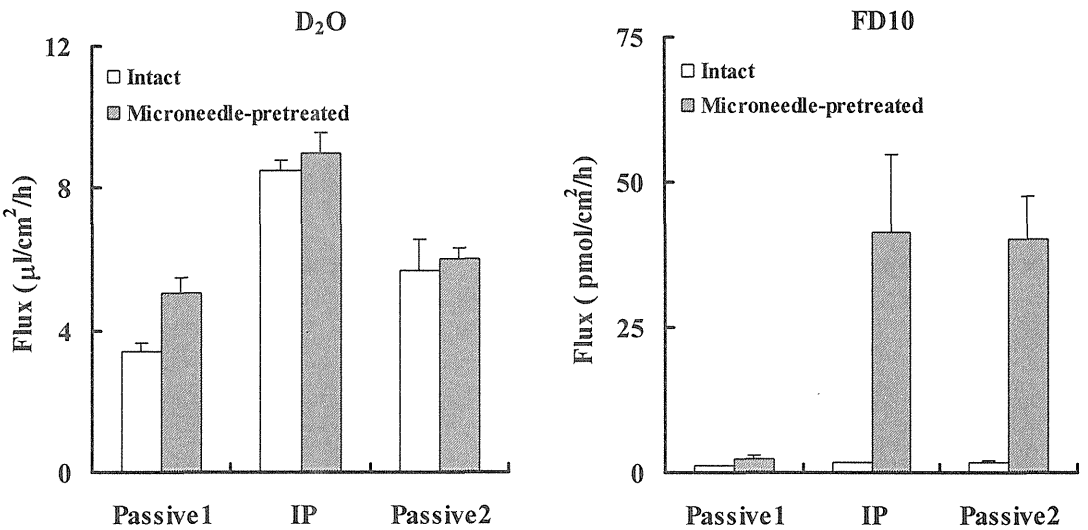


Fig. 2-4. Steady state flux of $D_2O$ or FD10 through intact and microneedle-pretreated hairless rat skin before (Passive1), during (IP) and after (Passive2) iontophoresis at 0.3 mA/cm$^2$. Left panel is $D_2O$, right panel is FD10.

Table 2-1 Steady state flux of $D_2O$ through hairless rat skin

| | Intact skin | Microneedle-pretreated skin |
|---|---|---|
| $Flux_{passive1}$ | 3.42 ± 0.23 | 5.07 ± 0.40 |
| $Flux_{IP}$ | 8.52 ± 0.29 | 9.01 ± 0.57 |
| $Flux_{passive2}$ | 5.67 ± 0.87 | 6.01 ± 0.31 |
| $Flux_{IP}$- $Flux_{passive2}$ | 2.86 (2.71) [a] | 3.00 (2.62) [a] |
| $Flux_{passive2}$/ $Flux_{passive1}$ | 1.65 | 1.19 |

[a] Values within parentheses were obtained from the capillary tube method

mean ± S.E. in μL/cm$^2$/h, n=3 or 4

Table 2-2 Steady state flux of FD10 through hairless rat skin.

| | Intact skin | Microneedle-pretreated skin |
|---|---|---|
| $Flux_{passive1}$ | 1.13 ± 0.09 | 2.30 ± 0.74 |
| $Flux_{IP}$ | 1.69 ± 0.24 | 41.52 ± 13.33 |
| $Flux_{passive2}$ | 1.80 ± 0.27 | 40.10 ± 7.64 |

mean ± S.E. in pmol/cm$^2$/h, n=3 or 4

Furthermore, post-iontophoresis passive flux of FD10 (passive2) was also high compared to iontophoresis flux during iontophoresis (IP) with microneedle pretreatment. One may easily consider it as a result of permeability factor, which is usually true for a small molecule. But here a large molecule was used as model penetrant. Firstly, if it were due to permeability factor, the same result of large $flux_{passive2}$ would be obtained for intact skin, too. Secondly, $flux_{IP}$, which contains the fluxes from electroosmotic transport and increased passive permeability, would be lager than $flux_{passive2}$ that only comes from increased passive permeability. Thirdly, 5h-preconditioning at the same iontophoresis conditions to microneedle-pretreated skin, the flux was compared to the $flux_{passive1}$ and not to the $flux_{passive2}$ (data not shown). So, permeability factor did not contribute significantly to $flux_{passive2}$. In fact, the high post-iontophoresis passive flux (passive2) is assumed to be a result of the low permeation of large molecules. In detail, large molecules penetrate through the stratum corneum and cannot be passed immediately through the epidermis and dermis during iontophoresis due to high molecule weight. After termination of the current, high passive flux continues from accumulated molecules in the epidermis and dermis.

*2.4.4. Combination effect of microneedle pretreatment and subsequent iontophoresis on the skin permeation of FDs*

The combination of microneedle pretreatment and iontophoresis further enhanced transdermal delivery of FD10. The obtained permeation behavior of FD10 was significantly different from that of $D_2O$. We then investigated the permeation profiles of FD4, 10, 40, 70 and 2000. The obtained results are shown in Figs. 2-5 and 2-6. No significant increase was found in the iontophoretic transport of FDs through intact skin; however, combination with microneedle pretreatment markedly increased the iontophoresis transport of FDs. Moreover, the cumulative amount of FDs that permeated through microneedle-pretreated skin showed a special behavior pattern, i.e., long lag time and large post-iontophoresis passive permeability. The lag time of FD4, FD10, FD40, FD70 and FD2000 was 0.36 h, 1.66 h, 1.17 h, 1.18 h and 2.82 h, respectively, which showed a tendency to being dependent on their molecular weight.

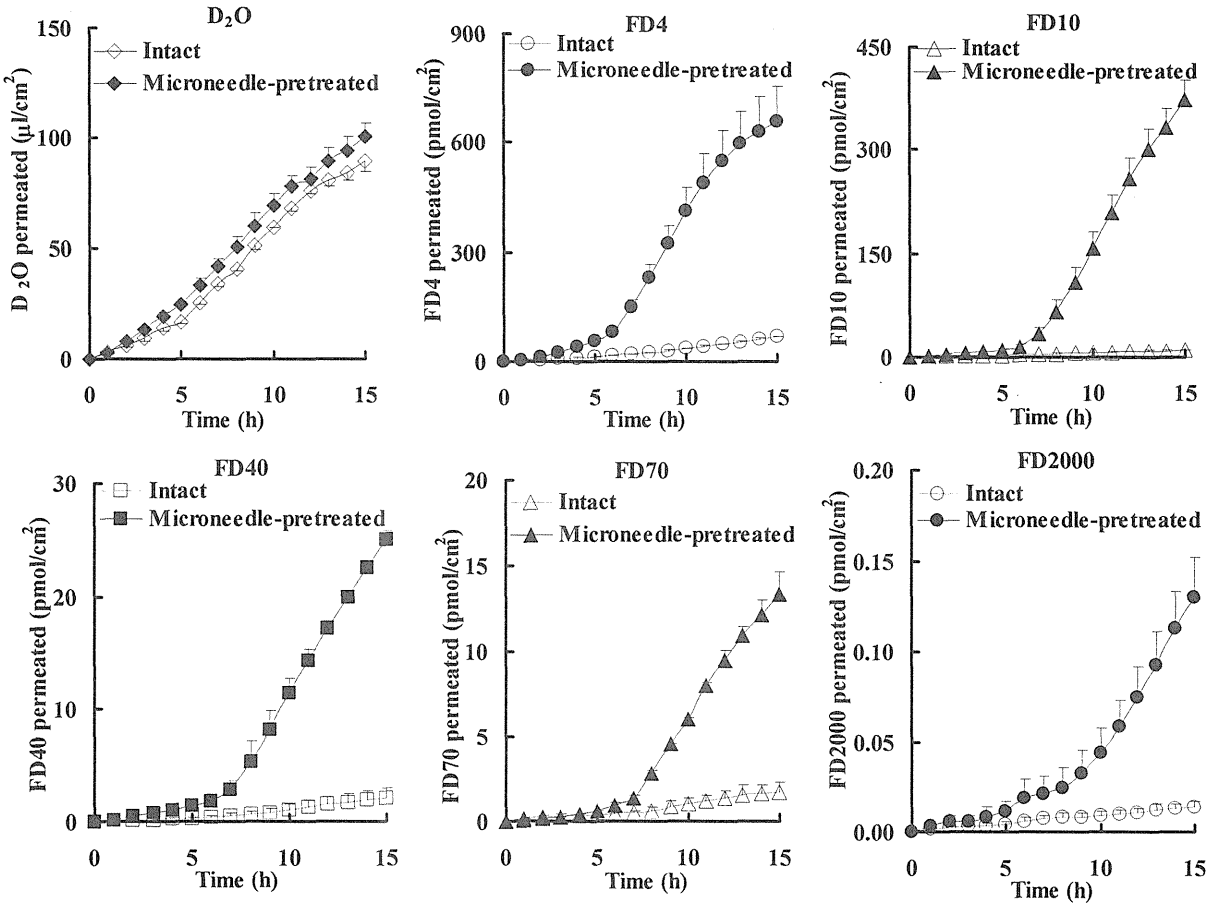


Fig. 2-5. Permeation of $D_2O$ and FDs through intact and microneedle-pretreated hairless rat skin before (0-5h), during (5-10h) and after (10-15h) iontophoresis at 0.3 mA/cm$^2$.

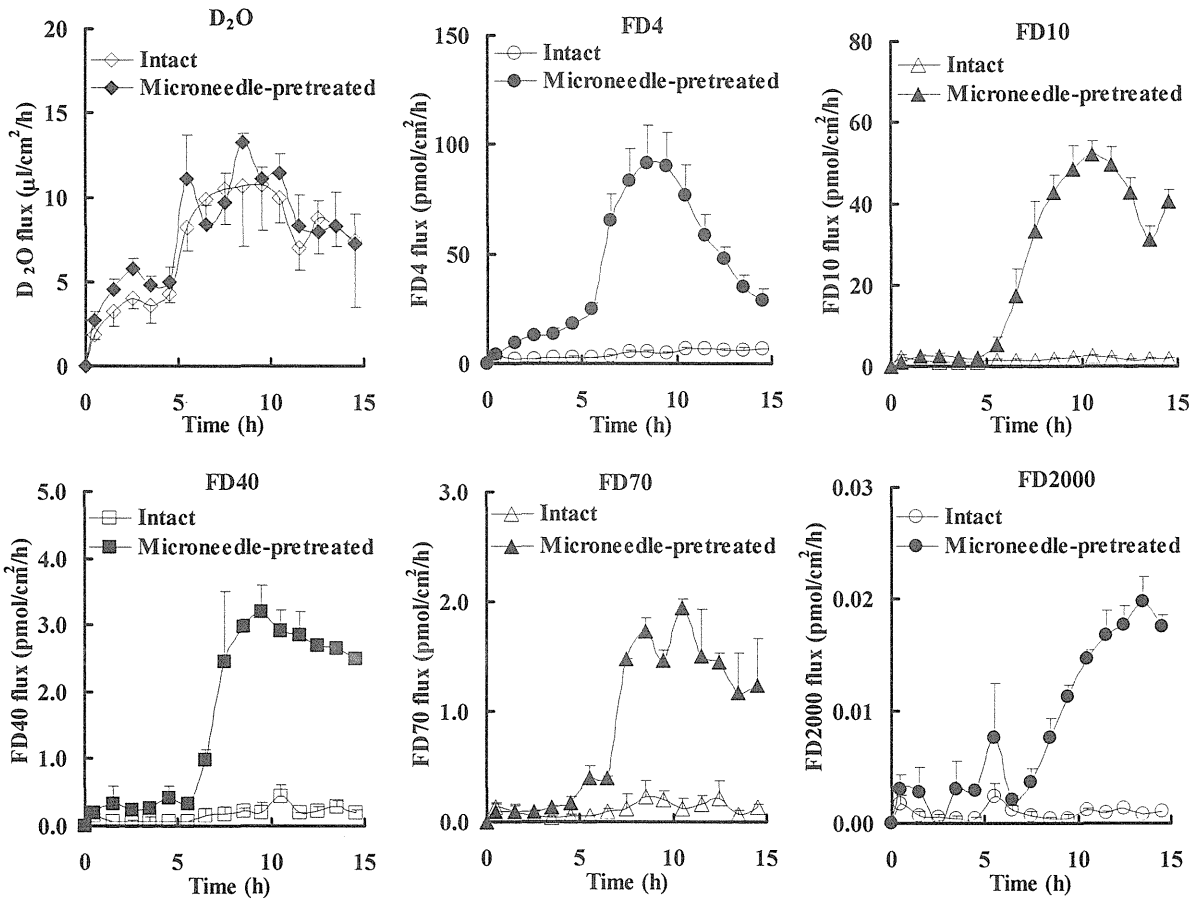


Fig. 2-6. Flux of $D_2O$ and FDs through intact and microneedle-pretreated hairless rat skin before (0-5h), during (5-10h) and after (10-15h) iontophoresis at 0.3 mA/cm$^2$.

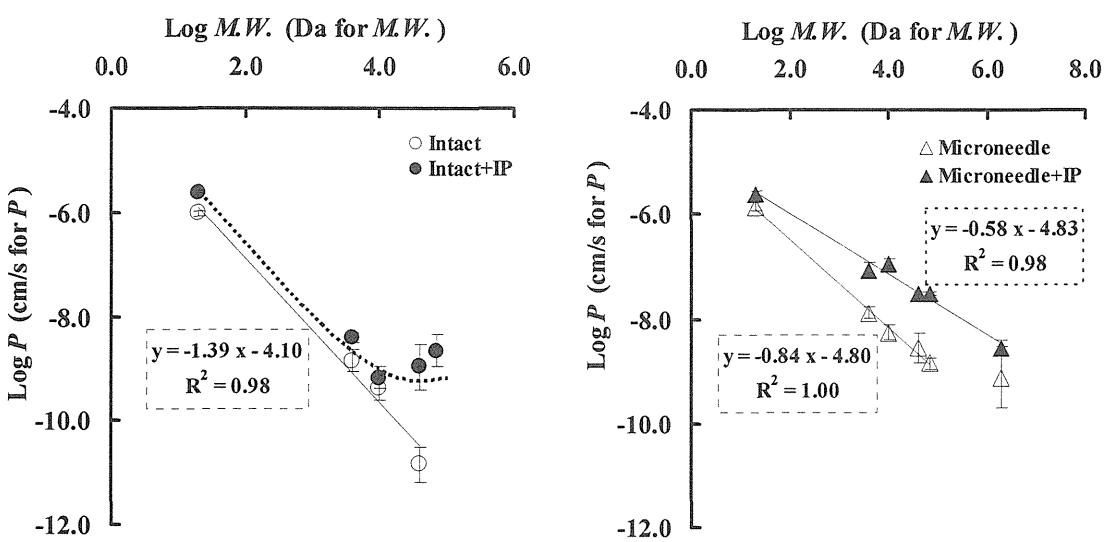


Fig. 2-7. Relationship between Log $P$ and Log $M.W.$ of $D_2O$ and FDs for intact and microneedle-pretreated hairless rat skin before and during iontophoresis at 0.3 mA/cm$^2$.

*2.4.5. Relationship between P and MW*

Furthermore, the relationship was evaluated between molecular weight (MW) and permeability coefficient (P) of the penetrants in the following four cases: passive permeability through intact skin (Intact), iontophoretic permeability through intact skin (Intact + IP), passive permeability through microneedle-pretreated skin (Microneedle), and iontophoretic permeability through microneedle-pretreated skin (Microneedle + IP). The results are shown in Fig. 2-7. Interestingly, relatively good linear correlations were observed between Log MW and Log P except for the Intact + IP. The contribution of iontophoresis to the enhancement of drug permeation through microneedle-pretreated skin increased with an increase in MW.

## 2.5. Chapter Conclusion

The present study demonstrated that physical pretreatment with microneedle puncture of the skin barrier, in conjunction with iontophoresis, can further enhance the transdermal delivery of high molecular compounds such as FD4, 10, 40, 70 and 2000. In contrast, microneedle pretreatment of the stratum corneum did not further increase the iontophoretic transport of $D_2O$. The combination of microneedle pretreatment and following iontophoresis provided a special skin permeation profile for large molecules, i.e., extended lag time and large post-iontophoresis passive permeability. Further investigation is necessary to more precisely control large molecule permeation by using microneedles with iontophoresis.

# Chapter 3

## Analysis of Enhanced Skin Permeation of Drugs Using Linear Phenomenological Equations

### 3.1. Introduction

A penetrant diffusion ($J$) through a membrane will be generated by a difference of chemical potential ($\Delta\mu$) from a side having high chemical potential to the opposite side in a closed transport system. Such a simple permeation phenomenon can be described by conventional equations such as Fick's law of diffusion. From a viewpoint of the biological physics on the material permeation through a membrane, $\Delta\mu$ is a "driving force" and $J$ is an obtained "flow"[55]. Generally, a system may contain several forces and flows, so that several interactions take place between nonconjugate forces and flows. Thus the conventional equations of solute and volume flows cannot completely describe all physical behavior of membranes. The linear phenomenological equations can be applied to analyze the permeation phenomena in these complex systems, which involve more than two forces and flows. Staverman[56] firstly used irreversible thermodynamics to treat membrane transport processes to completely solve the insufficiency of conventional equations on permeation phenomena. Then, in 1958 Kedem and Katchalsky further applied the formalism of non-equilibrium thermodynamics to biological membranes, and they successfully analyzed transport phenomena and derived the useful Kedem-Katchalsky equations from the linear phenomenological equations[57].

Primary driving forces of chemical potential differences of non-electrolyte FDs, water and ions, as well as an another driving force of voltage difference were applied across the skin in the present study on the combination of microneedle pretreatment and iontophoresis (Chapter 2). The transports of water and electrolyte were successfully described using a set of linear phenomenological equations when electrical potential was applied to a system containing only water and one permeable electrolyte through a membrane[58,59]. Nevertheless,

transport phenomena for more complex systems containing water, non-electrolytes and ions like the present experimental system have not been discussed. Then we try to analyze the *in vitro* skin permeation profiles of drugs using linear phenomenological equations. In the present experimental system, however, so many flows like flows of drugs, water and ions in PBS are involved, which making difficult to understand the system in detail. We then pay attention mainly to the drug permeation and try to explain to the contribution of passive diffusion and electroosmosis to the skin permeation of drugs by using the linear phenomenological equations.

## 3.2. Materials and Methods

The materials and methods used in this experiment were the same as described in Chapter 2.

## 3.3. Theoretical

### *3.3.1. Thermodynamics of irreversible processes and linear phenomenological equations in biological systems*

**Thermodynamics of irreversible processes** In order to describe the free energy change of a system in any irreversible process, it is often convenient to use the dissipation function, $\Phi$, which is defined by:

$$\Phi = T\left(\frac{dS}{dt}\right) \tag{1}$$

where $T$ is absolute temperature and $dS/dt$ is inner entropy change per unit time, $t$. For example, in a closed system at constant temperature and pressure, this function is equal to the rate of decrease (dissipation) of the Gibbs free energy ($-dG/dt$); more generally, it can always be related to the rate of dissipation of free energy or the rate of decrease in the ability to perform useful work.[55)]

Furthermore according to non-equilibrium principles, the dissipation function associated to entropy production may be also shown to the sum of products of flows $J_i$ and conjugated forces $X_i$ as shown below (where $i$ = 1, 2, 3, ……, n):

$$\Phi = \sum_{i}^{n} J_i X_i \tag{2}$$

where $J_i$ are flows of matter, heat, or electricity, and $X_i$ are generalized forces (conjugate forces) such as gradients of chemical potential, temperature, or electrical potential.

In the present study, the experimental system consists of two aqueous PBS solutions containing water, non-electrolyte FD and several salt ions separated by a skin membrane. The system thus comprises four driving forces and four flows: (1) the flow of FD, $J_s$, driven by the difference in the chemical potential, $\Delta\mu_s$, (2) the flow of water, $J_w$, driven by the difference in the chemical potential, $\Delta\mu_w$, (3) the flow of ions, $\Sigma J_{ion}$, driven by the difference in the electro-chemical potentials, $\Sigma\Delta\mu_{ion}$, and (4) the electrical current, $I$, driven by the voltage difference, $\Delta E$[57,58,59,60]. So the dissipation function for the flows of FDs, water, electrical current and ions can be expressed as follows:

$$\Phi = J_s\Delta\mu_s + J_w\Delta\mu_w + \sum J_{ion}\Delta\mu_{ion} + I\Delta E \tag{3}$$

According to thermodynamic expressions driving forces $\Delta\mu_s$, $\Delta\mu_w$ and $\Delta\mu_{ion}$ are:

$$\Delta\mu_s = \overline{V}_s\Delta P + \frac{\Delta\pi_s}{\dot{C}_s}$$

$$\Delta\mu_w = \overline{V}_w(\Delta P - \Delta\pi) = \overline{V}_w(\Delta P - \Delta\pi_s - \sum\Delta\pi_{ion})$$

$$\sum\Delta\mu_{ion} = \sum(\overline{V}_{ion}\Delta P + \frac{\Delta\pi_{ion}}{\dot{C}_{ion}}) \tag{4}$$

where $\overline{V}_s$, $\overline{V}_w$ and $\overline{V}_{ion}$ denote the partial molar volumes of FD, water and ions respectively, $\dot{C}_s$ and $\dot{C}_{ion}$ are the mean concentration of FD and ions in the two compartments[57], $\Delta P$ is the difference in pressure across the skin, $\Delta\pi$, $\Delta\pi_s$, $\Delta\pi_{ion}$ denote the difference in the osmotic pressure of the whole solution, FD and ions, and $\Delta E$ is t the voltage difference, respectively.

Introducing eqn. 4 into eqn. 3, the following equation can be written

$$\Phi = J_s(\overline{V}_s \Delta P + \frac{\Delta \pi_s}{\dot{C}_s}) + J_w \overline{V}_w (\Delta P - \Delta \pi) + \sum J_{ion}(\overline{V}_{ion} \Delta P + \frac{\Delta \pi_{ion}}{\dot{C}_{ion}}) + I \Delta E \quad (5)$$

The total volume flow, $J_v$, is related to the sum of FD, water and ions flows as follows:

$$J_v = J_s \overline{V}_s + J_w \overline{V}_w + \sum J_{ion} \overline{V}_{ion} \quad (6)$$

Denoting the volume fraction of FD and ions by $\varphi_s = \dot{C}_s \overline{V}_s$ and $\varphi_{ion} = \dot{C}_{ion} \overline{V}_{ion}$, the following eqn. 7 can be obtained from eqn. 5 and eqn. 6.[59)]

$$\Phi = J_s \frac{\Delta \pi_s}{\dot{C}_s}(1 + \varphi_s \frac{\Delta \pi}{\Delta \pi_s}) + J_v(\Delta P - \Delta \pi) + \sum J_{ion} \frac{\Delta \pi_{ion}}{\dot{C}_{ion}}(1 + \varphi_{ion} \frac{\Delta \pi}{\Delta \pi_{ion}}) + I \Delta E \quad (7)$$

In dilute solution $\varphi_s$ and $\varphi_{ion}$ are much less than unit, then eqn. 7 can be reduced to

$$\begin{aligned} \Phi &\doteq J_s \frac{\Delta \pi_s}{\dot{C}_s} + J_v(\Delta P - \Delta \pi) + \sum J_{ion} \frac{\Delta \pi_{ion}}{\dot{C}_{ion}} + I \Delta E \\ &= J_s(\frac{RT \Delta C_s}{\dot{C}_s}) + J_v(\Delta P - RT \Delta C) + \sum J_{ion}(\frac{RT \Delta C_{ion}}{\dot{C}_{ion}}) + I \Delta E \end{aligned} \quad (8)$$

**Linear phenomenological equations** In a simple system contains only a single force and a single flow, the flow is a linear function of the conjugated force over a relatively large range of flows and forces as shown below:

$$J_i = L_{ii} X_i \quad (9)$$

where $J_i$ is the flow, $X_i$ is the conjugate driving force, and $L_{ii}$ is a set of straight coefficients that relate the flow with its conjugate driving force. Fick's law of diffusion and Ohm's law of current flow are application examples of eqn. 9.

If there are more than two irreversible processes taking place, the flow $J_i$ is not only linearly related to its conjugate force $X_i$, but is also related to all other non-conjugate forces

found in the expression for dissipate function $\Phi$. Thus the linear phenomenological equations can be expressed as follows:

$$J_i = L_{ii}X_i + \sum_j^n L_{ij}X_j \tag{10}$$

where the $L_{ii}$ are straight coefficients as mentioned above and the $L_{ij}$ are coupling coefficients that relate the flows with non-conjugate driving forces.

Then, in the present experiments, the corresponding phenomenological equations are as follows according to eqn. 8 :

$$\begin{aligned}
J_s &= L_{ss}\frac{RT\Delta C_s}{\dot{C}_s} + L_{sv}(\Delta P - RT\Delta C) + \sum L_{si}\frac{RT\Delta C_{ion}}{\dot{C}_{ion}} + L_{sI}\Delta E \\
J_v &= L_{vs}\frac{RT\Delta C_s}{\dot{C}_s} + L_{vv}(\Delta P - RT\Delta C) + \sum L_{vi}\frac{RT\Delta C_{ion}}{\dot{C}_{ion}} + L_{vI}\Delta E \\
J_{ion} &= L_{is}\frac{RT\Delta C_s}{\dot{C}_s} + L_{iv}(\Delta P - RT\Delta C) + \sum L_{ii}\frac{RT\Delta C_{ion}}{\dot{C}_{ion}} + L_{iI}\Delta E \\
I &= L_{Is}\frac{RT\Delta C_s}{\dot{C}_s} + L_{Iv}(\Delta P - RT\Delta C) + \sum L_{Ii}\frac{RT\Delta C_{ion}}{\dot{C}_{ion}} + L_{II}\Delta E
\end{aligned} \tag{11}$$

$\Delta P$ and $\Delta C_{ion}$ are almost zero in the present study. Then, eqn. 11 can be reduced to

$$\begin{aligned}
J_s &= L_{ss}\frac{RT\Delta C_s}{\dot{C}_s} + L_{sv}(-RT\Delta C_s) + L_{sI}\Delta E \\
J_v &= L_{vs}\frac{RT\Delta C_s}{\dot{C}_s} + L_{vv}(-RT\Delta C_s) + L_{vI}\Delta E \\
J_{ion} &= L_{is}\frac{RT\Delta C_s}{\dot{C}_s} + L_{iv}(-RT\Delta C_s) + L_{iI}\Delta E \\
I &= L_{Is}\frac{RT\Delta C_s}{\dot{C}_s} + L_{Iv}(-RT\Delta C_s) + L_{II}\Delta E
\end{aligned} \tag{12}$$

We pay attention to the flux of FD, $J_s$, and may combine the coefficients of the first and second terms to a new coefficient, $\omega_s$, which is defined by[55,57]

$$\omega_s = \frac{L_{ss}}{\dot{C}_s} - L_{sv} \tag{13}$$

Then, $J_s$ can be simply expressed by

$$J_s = \omega_s RT\Delta C_s + L_{sI}\Delta E = P_{ss}\Delta C_s + L_{sI}\Delta E \quad (14)$$

From eqn. 14, FD flux, $J_s$, is found to be dependent on its conjugate force of concentration difference, $\Delta C_s$, as well as the non-conjugate force of voltage difference, $\Delta E$. When the coefficients $P_{ss}$ and $L_{sI}$ are determined, FD permeation can be completely described by eqn. 14.

On the other hand, the contribution of voltage difference, $\Delta E$, to the flux of non-electrolyte solute FD is present as solvent volume flow induced by electrical potential, i.e., electroosmosis. Thus the following equation can be obtained according to Kedem and Katchalsky[57]:

$$J_s = \omega_s RT\Delta C_s + (1-\delta)\times J_v \times \Delta C_s \quad (15)$$

where $\delta$ is reflection coefficient of the non-electrolyte penetrant. The reflection coefficient is an index showing the ability of the membrane to discriminate between the solute and solvent. $\delta = 1$ when the membrane is impermeable to solute, whereas $\delta = 0$ when the membrane is equally permeable to solute and solvent. The intermediate cases are $0 < \delta < 1$. Obviously, the reflection coefficient shows the contribution of convective flow to the total permeability of solute through the membrane.

*3.3.2. Mechanism of the combined effects of microneedle pretreatment and iontophoresis on the skin permeation of high molecular compounds*

We then use the reflection coefficient, $\delta$, to explain the mechanism of combined effects of microneedle pretreatment and iontophoresis on the skin permeation of high molechlar compounds. Figure 3-1 schematically illustrates electroosmotic transport for low and high molecular compounds before and after microneedle pretreatment. When the penetrant size is smaller than the permeation pores of skin, they can be dragged by solvent flow and permeated

through the membrane (i.e., $\delta \approx 0$), as shown in Fig. 3-1a. Although the microneedle pretreatment can make new pores in the membrane, the new pore pathway does not further contribute to the permeation of small molecules (Fig. 3-1b). On the other hand, large molecules cannot be permeated through the intact membrane together with solvent flow due to their large size (i.e., $\delta \approx 1$) (Fig. 3-1c). The production of new pores by microneedle pretreatment facilitates the passage of high molecular compounds through the membrane by decreasing the reflection coefficient, $\delta$ (Fig. 3-1d).

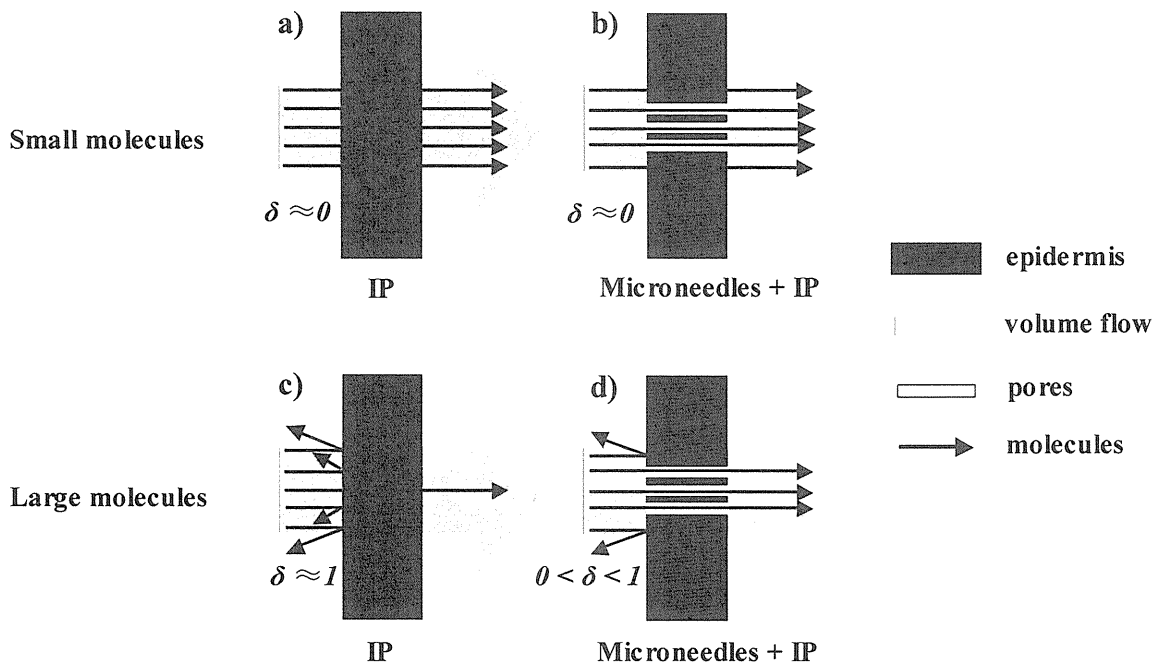


Fig. 3-1. Illustration of the permeation of small or large molecules through intact skin or microneedle-pretreated skin.

## 3.4. Results and Discussion

### *3.4.1. Measurement of the coefficients of $P_{ss}$ and $L_{sl}$ for FD4*

To determine a given coefficient, the system can be restricted to have only one force and corresponding flow. Then, the flow is determined under a single force and the coefficient is obtained from the ratio of flow to force.

In the present experiments, when the voltage difference is constant, i.e., $\Delta E$ =0, the coefficient $P_{ss}$ can be obtained from eqn. 14.

$$(\frac{J_s}{\Delta C_s})_E = P_{ss} \tag{16}$$

Relationship between the flux and concentration difference of FD4 is shown in Fig. 3-2a, and slope of the line is the $P_{ss}$. In a similar manner, when the concentration difference is constant, the coefficient $L_{sI}$ can be obtained from eqn. 14

$$(\frac{J_s}{\Delta E})_{\Delta C_s} = L_{sI} \tag{17}$$

The relationship between the flux of FD4 and electrical difference is shown in Fig. 3-2b, and slope of the line is the $L_{sI}$.

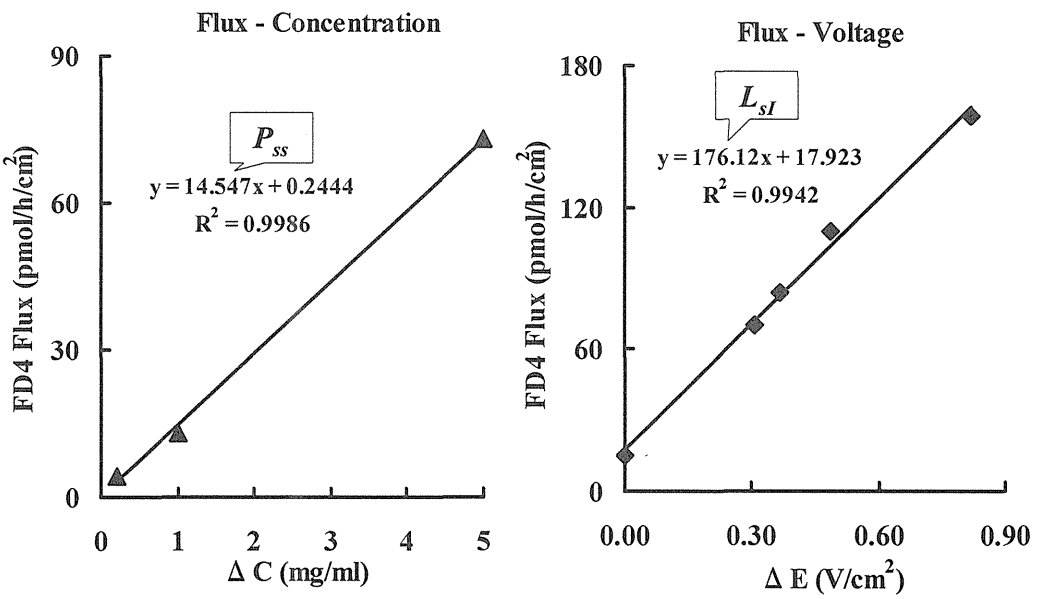


Fig. 3-2. Relationship between FD flux and concentration difference $\Delta C$ (a) or electrical difference $\Delta E$ (b). Slope of lines shows $P_{ss}$ and $L_{sI}$.

*3.4.2. Contribution of concentration difference of drugs and electroosmosis*

From eqn. 14, the total drug flux, $J_s$, consists of $P_{ss}\Delta C_s$ and $L_{sI}\Delta E$, where the former is for passive diffusion and the latter is for electroosmosis produced by iontophoresis. Table 3-1 summarizes the contribution of concentration difference of drugs and electroosmosis before and after microneedle pretreatment. For the intact skin, the electroosmosis induced

by the electrical power did not have a big contribution to the skin permeation of high molecular weight compounds. On the other hand, the electroosmosis significantly enhanced the skin permeation of penetrants, and the contribution of electoosmosis increased with an increase in M.W. of the penetrants.

Table 3-1 Fluxes of $D_2O$ and FDs and contribution of concentration difference of drugs and electroosmosis before and after microneedle pretreatment

| Drugs | Intact skin | | Microneedle-pretreated skin | |
|---|---|---|---|---|
| | $P_{ss}\Delta C_s$[a] | $L_{sl}\Delta E$[b] | $P_{ss}\Delta C_s$[a] | $L_{sl}\Delta E$[b] |
| $D_2O$ | $3.4 \times 10^6$ (40%)[c] | $5.1 \times 10^6$ (60%) | $5.1 \times 10^6$ (56%) | $3.9 \times 10^6$ (44%) |
| FD4 | 5 (36%) | 9 (64%) | 47 (15%) | 267 (85%) |
| FD10 | Very low | Very low | 20 (5%) | 395 (95%) |
| FD40 | Very low | Very low | 10 (9%) | 100 (9%) |
| FD70 | Very low | Very low | 5 (5%) | 103 (95%) |

[a] $\Delta C_s$ of FDs was fixed to be 1.0 mg/mL, and pure $D_2O$ was used in all experiments.

[b] $\Delta E$ was fixed to be 0.4 V.

[c] Values within parentheses are permeation ratios compared to the total permeation.

mean ± S.E. in ng/cm$^2$/h, n=3 or 4

*3.4.3. Pretreatment effect of microneedles on the skin permeation of $D_2O$ and FDs*

The reflection coefficient[56,57], $\delta$, is closely related to the contribution of convective flow to the total permeability of solute through the skin barrier. This parameter is very important to iontophoretic flux-enhancement for large molecules. Then, the different effects of microneedle pretreatment were evaluated using $\delta$ value on the iontophoretic flux of $D_2O$ and FDs in Chapter 2. After the pretreatment, no significant increase was observed in the electroosmotic transport of $D_2O$. Since the reflection coefficient $\delta$ of $D_2O$ to solvent flux ($\delta$ = 0 in both cases, see Fig. 3-1a and b) and solvent volume flow before microneedle pretreatment were almost the same as those after the pretreatment, little difference was observed in the electroosmotic transport of $D_2O$ before and after pretreatment.

On the other hand, microneedle pretreatment significantly increased the electroosmotic transport of FDs because of the significant decrease in $\delta$ (see Fig. 3-1c and d).

*3.4.4. Pretreatment effect of microneedles on the $\delta$ of FDs*

Furthermore, the $\delta$ values of FDs in the iontophoresis experiment before and after microneedle pretreatment were investigated. Compared to electroosmotic transport, passive1 flux is negligible, so $\delta$ can be expressed from eqn. 15 as follows:

$$\delta = 1 - \frac{Flux}{J_v \times \Delta C_s} \tag{18}$$

The obtained results are shown in Fig. 3-3. The δ values of FDs for intact skin were close to unit. After the pretreatment with microneedles, on the other hand, the $\delta$ values were significantly decreased, which may be due to synergistic effects of microneedle pretreatment and subsequent iontophoresis on the skin permeation of large molecules.

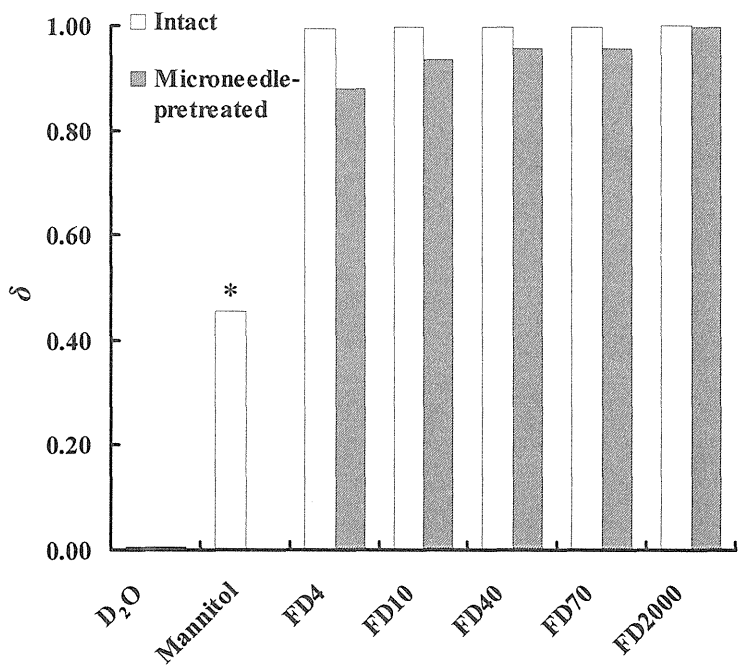


Fig. 3-3 $\delta$ of penetrants with different molecular weight for intact and microneedle-pretreated hairless rat skin during iontophoresis at 0.3 mA/cm$^2$.

* Data adapted from Kim et al[61]. Iontophoresis condition: constant current 0.36 mA/cm$^2$, and other conditions were the same to the present study.

### 3.5. Chapter Conclusion

Linear phenomenological equations were useful for clear understanding and explanation of the contribution of passive diffusion and electroosmosis to the skin permeation of drugs. Through applying the concept of reflection coefficient, $\delta$, to the present skin permeation experiments, a reasonable explanation was obtained for the mechanism of the combined effects of microneedle pretreatment and iontophoresis on the skin permeation of high molecular compounds.

When more than two forces and flows involved in a system, the linear phenomenological equations can provide a useful approach to analyze the complex permeation phenomena.

## Conclusion

From these results obtained above, the following conclusion can be obtained:

(1) The microneedle pretreatment may provide a safe, efficient and controllable technique for increasing transdermal drug delivery. Especially microneedle system can provide a technique platform for transdermal delivery of hydrophilic high molecular weight compounds, such as proteins and DNA.

(2) A combination of microneedle and iontophoresis further increases skin permeation of hydrophilic high molecular weight compounds. The combination approach can expand the range of drugs suitable for transdermal delivery.

(3) When a transport system contains more than two driving forces, for example, just like the drugs skin permeation of a combination of microneedle and iontophoresis, the linear phenomenological equations can provide a useful approach to analyze the complex penetrant permeation phenomena. It was useful for clear understanding and explanation of the contribution of each driving force, i.e., passive diffusion (concentration difference) and electroosmosis (electrical potential difference), to the skin permeation of drugs.

Microneedle system and its combination system with iontophoresis may be useful to increase the skin permeation of high molecular weight compounds. Application of resistance model and linear phenomenological equations are useful to sophisticatedly fabricate a microneedle system. The present system can be utilized as a new drug delivery means through skin.

## Acknowledgement

It is a pleasure to thank many people who made this thesis possible.

I would like to express my sincere gratitude to my Ph.D. supervisor, Professor Kenji Sugibayashi (Department of Clinical Pharmacokinetics, Faculty of Pharmaceutical Sciences, Josai University). With his enthusiasm, his inspiration, and his great efforts to explain things clearly and simply, he helped to make research work fun for me. Throughout my thesis-writing period, he provided encouragement, sound advice, good teaching, philosophy thinking, and lots of good ideas. I would have been lost without him.

I am also like to thank Assistant Dr. Hiroaki Todo, Assistant Mr. Hiroshi Ishii and Dr. Nobuko Hada for their valuable discussion through the present research.

I am especially grateful to Mr. Tomoyuki Mitoma, Mr. Hirotaka Yasuno, Mr. Koichi Honda, Mr. Toshihiko Kitamura, Mr. Murayama Kazuhiro, Mr. Iino Takao and Ms. Satoko Sugasawa, for helping me overcome the communication barrier, get through the difficult times, and for all the emotional support, camaraderie, entertainment, and caring they provided in my daily life in Japan. I also wish to thank all other colleagues who have helped me.

Also, I am grateful to Professor Weisan Pan (Shenyang Pharmaceutical University, China) for his understanding, supporting, and giving me this opportunity to go to Japan to carry out the present study.

Lastly, and most importantly, I am forever indebted to my parents. They bore me, raised me, supported me, taught me, and loved me. I also wish to express my deep gratitude to my wife for her continual love, kindly encouragement, and endless support.

## References


1. A.C. Williams, B.W. Barry, Penetration enhancers, Adv. Drug Deliv. Rev. 56 (2004) 603-618.
2. Y.N. Kalia, A. Naik, J. Garrison, R.H. Guy, Iontophoretic drug delivery, Adv. Drug Deliv. Rev. 56 (2004) 619-658.
3. A.R. Denet, R. Vanbever, V. Preat, Skin electroporation for transdermal and topical delivery, Adv. Drug Deliv. Rev. 56 (2004) 659-674.
4. M.R. Prausnitz, S. Mirtagotri, R. Langer, Current status and future potential of transdermal drug delivery, Nat. Rev. Drug Discov. 3 (2004) 115-124.
5. S. Mitragotri, J. Kost, Low-frequency sonophoresis: a review, Adv. Drug Deliv. Rev. 56 (2004) 589-601.
6. D.V. McAllister, P.M. Wang, S.P. Davis, J.H. Park, P.J. Canatella, M.G. Allen, M.R. Prausnitz, Microfabricated needles for transdermal delivery of macromolecules and nanoparticles: fabrication methods and transport studies, Proc. Nat. Acad. Sci. USA. 100 (2003) 13755-13760.
7. S. Kaushik, A.H. Hord, D.D. Denson, D.V. McAllister, S. Smitra, M.G. Allen, M.R. Prausnitz, Lack of pain associated with microfabricated microneedles, Anesth. Analg. 92 (2001) 502-504.
8. Y.W. Chien, A.K. Banga, Iontophoretic (transdermal) delivery of drugs: overview of historical development, J. Pharm. Sci. 78 (1989) 353-354.
9. N. Abla, A. Naik, R.H. Guy, Y.N. Kalia, 2006. Iontophoresis: clinical applications and future challenges, in Percutaneous Penetration Enhancers, 2nd ed. eds. by E.W. Smith, H.I. Maibach, CRC press. Taylor & Francis Group. 14, 177-219.
10. J.E. Riviere, N.A. Moteiro-Riviere, R.A. Rogers, D. Bommannan, J.A. Tamada, R.O. Potts, Pulsatile transdermal delivery of LHRH using electroporation: drug delivery and skin toxicology, J. Control. Release 36 (1995) 229–233.
11. S.L. Chang, G.A. Hofmann, L. Zhang, L.J. Deftos, A.K. Banga, The effect of electroporation on iontophoretic transdermal delivery of calcium regulating hormones, J.

Control. Release 66 (2000) 127–133.

12. S. Tokumoto, K. Mori, N. Higo, K. Sugibayashi, Effect of electroporation on the electroosmosis across hairless mouse skin *in vitro*, J. Control. Release 105 (2005) 296–304.
13. L. Le, J. Kost, S. Mitragotri, Combined effect of low-frequency ultrasound and iontophoresis: applications for transdermal heparin delivery, Pharm. Res. 17 (2000) 1151-1154
14. D.B. Bommannan, J. Tamada, L. Leung, R.O. Potts, Effect of electroporation on transdermal iontophoretic delivery of luteinizing hormone releasing hormone (LHRH) *in vitro*, Pharm. Res. 11 (1994) 1809-1814
15. J.Y. Fang, T.L. Hwang, Y.B. Huang, Y.H. Tsai, Transdermal iontophoresis of sodium nonivamide acetate. V. Combined effect of physical enhancement methods, Int. J. Pharm. 235 (2002) 95–105.
16. H.D. Smyth, G. Becket, S. Mehta, Effect of permeation enhancer pretreatment on the iontophoresis of luteinizing hormone releasing hormone (LHRH) through human epidermal membrane (HEM), J. Pharm. Sci. 91 (2002) 1296–1307.
17. Y. Wang, L.V. Allen Jr., L.C. Li, Effect of sodium dodecyl sulfate on iontophoresis of hydrocortisone across hairless mouse skin, Pharm. Dev. Technol. 5 (2000) 533–542.
18. O. Pillai, V. Nair, R. Panchagnula, Transdermal iontophoresis of insulin: IV. Influence of chemical enhancers, Int. J. Pharm. 269 (2004) 109–120.
19. K. Sugibayashi, M. Kagino, S. Numajiri, N. Inoue, D. Kobayashi, M. Kimura, M. Yamaguchi, Y. Morimoto, Synergistic effects of iontophoresis and jet injector pretreatment on the *in-vitro* skin permeation of diclofenac and angiotensin II, J. Pharm. Pharmacol. 52 (2000) 1179-1186.
20. Y. Wang, R. Thakur, Q. Fan, B. Michniak, Transdermal iontophoresis: combination strategies to improve transdermal iontophoretic drug delivery, Eur. J. Pharmaceut. Biopharm. 60 (2005) 179-191.
21. X.M. Wu, H. Todo, K. Sugibayashi, Effects of pretreatment of needle puncture and sandpaper abrasion on the *in vitro* skin permeation of fluorescein isothiocyanate

(FITC)-dextran, Int. J. Pharm. 316 (2006) 102-108.

22. X.M. Wu, H. Todo, K. Sugibayashi, Enhancement of skin permeation of high molecular weight compounds by combination of iontophoresis and acupuncture needle pretreatment, J. Control. Release (2007) in press.
23. S. Henry, D.V. McAllister, M.G. Allen, M.R. Prausnitz, Microfabricated microneedles: a novel approach to transdermal drug delivery, J. Pharm. Sci. 87 (1998) 922-925.
24. M.R. Prausnitz, Microneedles for transdermal drug delivery, Adv. Drug Deliv. Rev. 56 (2004) 581-587.
25. M. Cormier, B. Johnson, M. Ameri, K. Nyam, L. Libiran, D.D. Zhang, P. Daddona, Transdermal delivery of desmopressin using a coated microneedle array patch system, J. Control. Release 97 (2004) 503-511.
26. J.G.E. Gardeniers, R. Luttge, J.W. Berenschot, M.J. deBoer, Y. Yeshurun, M. Hefetz, R. van'tOever, A. van den Berg, Silicon micromachined hollow microneedles for transdermal liquid transport, J. Microelectromech. Syst. 12 (2003) 855-861.
27. R.K. Sivamani, B. Stoeber, G.C. Wu, H. Zhai, D. Liepmann, H. Maibach, Clinical microneedle injection of methyl nicotinate: stratum corneum penetration, Skin Res. Technol. 11 (2005) 152-156.
28. Y. Li, R. S. Shawgo, B. Tyler, P. T. Henderson, J. S. Vogel, A. Rosenberg, P. B. Storm, R. Langer, H. Brem, M. J. Cima, *In vivo* release from a drug delivery MEMS device, J. Control. Release 100 (2004) 211-219.
29. W. Martanto, S.P. Davis, N.R. Holiday, J. Wang, H.S. Gill, M.R. Prausnitz, Transdermal delivery of insulin using microneedles *in vivo*, Pharm. Res. 21 (2004) 947-952.
30. S.P. Davis, W. Martanto, M.G. Allen, M.R. Prausnitz, Hollow metal microneedles for insulin delivery to diabetic rats, IEEE Trans. Biomed. Eng. 52 (2005) 909-915.
31. M.A. Teo, C. Shearwood, K.C. Ng, J. Lu, S. Moochhala, *In vitro* and *in vivo* characterization of MENS microneedles, Biomed. Microdevices. 7 (2005) 47-52.
32. J.H. Park, M.G. Allen, M.R. Prausnitz, Biodegradable polymer microneedles; fabrication, mechanics and transdermal drug delivery, J. Control. Release 104 (2005) 51-66.
33. J.A. Matriano, M. Cormier, B. Johnson, W.A. Yong, M. Buttery, K. Nyam, P.E. Daddona,

Macroflux® microprojection array patch technology: a new and efficient approach for intracutaneous immunization, Pharm. Res. 19 (2002) 63-70.

34. W.Q. Lin, M. Cormier, A. Samiee, A. Griffin, B. Johnson, C.L. Teng, G.E. Hardee, P.E. Daddona, Transdermal delivery of antisense oligonucleotides with microprojection patch (Macroflux®) technology, Pharm. Res. 18 (2001) 1789-1793.
35. J.A. Mikszta, J.B. Alarcon, J.M. Brittingham, D.E. Sutter, R.J. Pettis, N.G. Harvey, Improved genetic immunization via micromechanical disruption of skin-barrier function and targeted epidermal delivery, Nat. Med. 8 (2002) 415-419.
36. F. Chabri, K. Bouris, T. Jones, D. Barrow, A. Hann, C. Allender, K. Brain, J. Birchall, Cutaneous biology microfabricated silicon microneedles for nonviral cutaneous gene delivery, Br. J. Dermatol. 150 (2004) 869-877.
37. R.C. Scott, P.H. Dugard, A.W. Doss, Permeability of abnormal rat skin, J. Invest. Dermatol. 86 (1986) 201-207.
38. S. Messager, A.C. Hann, P.A. Goddard, P.W. Dettmar, J.Y. Maillard, Assessment of skin viability: is it necessary to use different methodologies? Skin Res. Technol. 9 (2003) 321-330.
39. Y. Tokudome, K. Sugibayashi, The synergic effects of various electrolytes and electroporation on the *in vitro* skin permeation of calcein, J. Control. Release 92 (2003) 93-101.
40. R.W. Baker, H.K. Lonsdale, Controlled release: mechanisms and rates, in Advances in Experimental Medicine and Biology, eds. by Tanquary and Lacey, R.E., Plenum Press. New York and London. 47 (1974) 15-71.
41. R.J. Scheuplein, Mechanism of percutaneous absorption. II. Transient diffusion and the relative importance of various routes of skin penetration. J. Invest. Dermatol. 48 (1967) 79-88.
42. Y.N. Kalia, A. Naik, J. Garrison, R.H. Guy, Iontophoretic drug delivery, Adv. Drug Deliv. Rev. 56 (2004) 619-658.
43. M.R. Prausnitz, V.G. Bose, R. Langer, J.C. Weaver, Electroporation of mammalian skin: a mechanism to enhance transdermal drug delivery, Proc. Natl. Acad. Sci. U. S. A. 90

(1993) 10504-10508.

44. S. Mitragotri, D. Blankschtein, R. Langer, Ultrasound-mediated transdermal protein delivery, Science 269 (1995) 850-853.
45. M.J. Pikal, The role of electroosmotic flow in transdermal iontophoresis, Adv. Drug Deliv. Rev. 46 (2001) 281-305.
46. B. Kari, Control of blood glucose levels in alloxan-diabetic rabbits by iontophoresis of insulin, Diabetes 35 (1986) 217-221.
47. N. Kanikkannan, J. Singh, P. Ramarao, Transdermal iontophoretic delivery of bovine insulin and monomeric human insulin analogue, J. Control. Release 59 (1999) 99-105.
48. N. Abla, A. Naik, R.H. Guy, Y.N. Kalia, Contributions of electromigration and electroosmosis to peptide iontophoresis across intact and impaired skin, J. Control. Release 108 (2005) 319-330.
49. A.C. Hirsch, R.S. Upasani, A.K. Banga, Factorial design approach to evaluate interactions between electrically assisted enhancement and skin stripping for delivery of tacrine, J. Control. Release 103 (2005) 113-121.
50. M.J. Pikal, S. Shah, Transport mechanisms in iontophoresis. II. Electroosmotic flow and transference number measurements for hairless mouse skin, Pharm. Res. 7 (1990) 213-221.
51. Y. Kobatake, M. Yuasa, H. Fujita, Studies of membrane phenomena. VI. Further study of volume flow, J. Phys. Chem. 72 (1968) 1752-1757.
52. T. Hatanaka, E. Manabe, K. Sugibayashi, Y. Morimoto, An application of the hydrodynamic pore theory to percutaneous absorption of drugs, Pharm. Res. 11 (1994) 654-658.
53. N.H. Yoshida, M.S. Roboerts, Solute molecular size and transdermal iontophoresis across excised human skin, J. Control. Release 25 (1993) 177-195.
54. R.H. Guy, Y.N. Kalia, M.B. Delgado-Charro, V. Merino, A. Lopez, D. Marro, Iontophoresis: electrorepulsion and electroosmosis, J. Control. Release 64 (2000) 129-132.
55. S.G. Schultz, 1980. Basic principles of membrane transport, Cambridge University Press,

Cambridge 1980, 57-73.

56. A.J. Staverman, The theory of measurement of osmotic pressure, Rec. Trav. Chim. 70 (1951) 344-352.
57. O. Kedem, A. Katchalsky, Thermodynamic analysis of the permeability of biological membranes to non-electrolytes, Biochim. Biophys. Acta 27 (1958) 229-246.
58. I. Michaeli, O. Kedem, Description of the transport of solvent and ions through membranes in terms of differential coefficients Part 1.- Phenomenological characterization of flows, Trans. Faraday Soc. 57 (1961) 1185-1190.
59. O. Kedem, A. Katchalsky, Permeability of composite membranes Part 1.- Electric current, volume flow and flow of solute through membranes, Trans. Faraday Soc. 59 (1963a) 1918-1930.
60. A. Katchalsky, O. Kedem, Thermodynamics of flow processes in biological systems, Biophys. J. 2 (1962) 53-78.
61. A. Kim, P.G. Green, G. Rao, R.H. Guy, Convective solvent flow across the skin during inotophoresis, Pharm. Res. 10 (1993) 1315-1320.